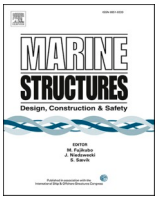
Marine Structures 112 (2027) 104256



Contents lists available at ScienceDirect

Marine Structures

journal homepage: www.elsevier.com/locate/marstruc



Research Paper

Adhesive bonding for stiffening thin-walled steel structures in shipbuilding applications: Experimental and numerical investigation of the bending capacity

Jannis Damm [a,*], Peter Haase [a], Matthias Albiez [a], Thomas Ummenhofer [a], Sebastian Veller [b]

[a] Karlsruhe Institute for Technology (KIT), Research Center for Steel, Timber and Masonry, Karlsruhe, Germany
[b] Fraunhofer Institute for Manufacturing Technology and Advanced Materials IFAM, Bremen, Germany

ARTICLE INFO

Keywords:
Structural adhesive bonding
Maritime steel construction
Shipbuilding
Stiffened panel structures
Shop-primer

ABSTRACT

This paper investigates the potential of structural adhesive bonding as an innovative joining technology for maritime steel construction, with a focus on shipbuilding and offshore applications. The study encompasses the selection and characterization of suitable adhesive systems and steel substrates, including the influence of protective shop primers. Experimental and numerical analyses are performed on plate components stiffened with both one and three stiffener profiles to evaluate the mechanical performance of adhesively bonded joints for ship building. Findings demonstrate that adhesive bonding can achieve high load-bearing capacities and maintain structural integrity. Furthermore, adhesive joining preserves the integrity of protective coatings and can simplify manufacturing processes where primer adhesion is verified by reducing the need for additional surface preparation and post-processing typical of welding. The results provide practical recommendations for surface pretreatment, adhesive selection, and process integration in shipyards, contributing to the wider adoption of adhesive technology in primary and secondary ship structures. Overall, the work highlights adhesive bonding as a viable alternative or supplement to conventional joining methods, supporting increased design flexibility, corrosion protection, and sustainable production in the maritime industry.

1. Introduction

Recent advancements have highlighted structural adhesive bonding as an innovative joining solution for shipbuilding and offshore engineering. Unlike established methods such as welding, riveting, or mechanical fastening, adhesive bonding introduces significant benefits. It minimises stress concentrations, preserves essential protective coatings, and avoids the thermal distortions commonly associated with welding procedures [1,2]. The adoption of adhesives can also lead to lighter structures, superior corrosion resistance, and greater manufacturing flexibility, advantages that become particularly relevant in areas that are challenging to access or where conventional tools are impractical [3]. Additionally, adhesive bonding enables the combination of dissimilar materials, thus expanding design options and facilitating the realization of advanced hybrid constructions [4].

From a sustainability perspective, adhesive joining is equally promising. It supports efficient maintenance strategies, including

* Corresponding author.
E-mail address: jannis.damm@kit.edu (J. Damm).

https://doi.org/10.1016/j.marstruc.2026.104256
Received 28 July 2026; Received in revised form 1 October 2026; Accepted 10 October 2026
Available online 26 October 2026
0951-8339/© 2026 The Author(s). Published by Elsevier Ltd. This is an open access article under the CC BY license (http://creativecommons.org/licenses/by/4.0/).
Open access funding enabled and organized by Projekt DEAL.

repair, refurbishment, and the possibility of reuse following a subsequent debonding process [5,6], all of which contribute to more environmentally responsible maritime practices [7,8] and the reduction of energy demand and greenhouse gas emissions [9].

Traditional joining processes in ship construction frequently encounter difficulties when dealing with coated, certified surfaces aimed at ensuring optimal adhesion, longevity, environmental resilience, and corrosion resistance [10]. Welding or fastening on such substrates usually mandates removal of protective layers, extensive pre-treatment, execution of joining, and subsequent restoration of the coating for corrosion protection, often followed by re-certification. In contrast, adhesive bonding allows for the direct attachment of parts onto intact coated surfaces, reducing overall process complexity and curtailing both maintenance needs and operational downtime [10].

A major factor in the assembly process is the use of shop primers, which serve as thin anti-corrosion layers applied to steel components ahead of fabrication. Designed to dry rapidly while remaining weldable and suitable for further processing, these primers, commonly zinc silicate or, alternatively, epoxy-based, either stay on as a primer for later coatings or are partially removed, as determined by specific coating protocols [11].

The durability of adhesively bonded joints employed in marine settings is subject to a variety of environmental and mechanical influences, such as cyclic temperature changes, persistent moisture, long-term immersion in seawater, salt spray, and continuous loads [12,13]. Resistance to aggressive chemicals, including solvents and substances employed for maintenance, is also required to preserve the integrity of bonded connections over extended periods [1,14]. Research has established that, across numerous investigations [15–19] unsealed adhesive joints in metals generally suffer from diminished mechanical capability after prolonged exposure to marine conditions.

Remarkably, even though industry interest in adhesive bonding for coated steel substrates is growing, only a handful of studies have investigated the long-term behaviour of such joints in shipbuilding. These studies are almost exclusively conducted on coupon-scale specimens (e.g., single- or double-lap joints). Durability data for adhesively bonded steel structures at component scale, comprising bond areas and stiffener lengths in the order of metres, are, to the authors' knowledge, not yet available. Research on adhesive bonding of large-scale, load-bearing steel structures is therefore still at an early stage, and the transferability of coupon-level durability results to such structures has not been established.

In some cases, the presence of sodium chloride has been observed to improve both the static and fatigue life of epoxy-bonded painted steel, as moisture-induced diffusion helps alleviate stress concentrations at overlap extremities, so enhancing the strength of inherently rigid adhesives [20]. Research reported in [21] found that polyurethane adhesive bonds, applied to epoxy- and polysiloxane-coated surfaces, retained their deformation behaviour even after artificial marine ageing tests. Furthermore, experimental results suggest that adhesives suitable for underwater curing can achieve reliable load transfer in stud bonding, with optimal coating systems further enhancing performance under simulated seawater exposure [2].

1.1. Stiffening of steel plates subjected to bending stresses in shipbuilding and steel construction

Due to the low bending stiffness of thin-walled components, stiffening elements (also known as stiffeners) are often required to minimise deformation and increase load-bearing capacity. The stiffening elements serve to increase shear and bending stiffness, as well as buckling resistance [22]. The stiffeners can be attached either by mechanical fasteners, welding or adhesive bonding [23]. Stiffened flat structural elements are found in a wide variety of fields, including shipbuilding [24], aircraft construction [25], orthotropic slabs in bridge construction [26] and lock gates [27,28]. In the case of large-area steel components in shipbuilding and hydraulic engineering, the stiffening elements are usually attached by welding. This involves creating linear welded joints between the stiffener and the (deck) plate. However, this type of joint is associated with harmful heat input, which can have a negative effect on the dimensional stability of the components. Furthermore, the induced residual welding stresses and notches can increase the risk of failure and, in particular, reduce fatigue strength.

1.2. The use of adhesive technology in shipbuilding and other industries of mechanical engineering

In maritime steel construction, stiffening elements have so far been fastened predominantly by welding. By contrast, adhesive bonding is already standard practice for numerous joints in other industries. The requirements in terms of stress, service life, environmental conditions and manufacturing are similar in many respects to those in shipbuilding. In the automotive industry, for example, an average of around 20 kg of adhesive has been used per vehicle for years, with the majority being applied to steel joints or composite structures in bodywork construction. Adhesive bonding of stiffeners is also used in aircraft construction. Structural bonding has been used in this sector for more than fifty years to attach external sheet metal stiffeners to the fuselage, airframe, wings and tail [29]. In aviation, the focus is particularly on lightweight construction combined with high strength and durability. Similar developments can also be seen in rail vehicle construction, where industrial bonding is widely used. The DIN 6701 standard provides a uniform normative basis in this field [30]. Additionally, the wind energy sector should be mentioned, where structural bonding is widely used, particularly for rotor blades [31].

In boat and yacht building, adhesive bonding is used for joints subject to lower stress, such as when fitting deck profiles and deck coverings, as well as for deck superstructures such as flybridge constructions, windows and interior fittings [32,33]. Deck-to-hull and keel-to-hull bonding are also common in yacht building [34].

In shipbuilding, by contrast, welded and bolted steel structures remain the established standard. Apart from glass bonding, adhesive bonding has so far only been used in the assembly of equipment components such as pipe supports or cable trays. Overall, the bonding process has so far been of secondary importance compared to welding. However, structural adhesive joints in shipbuilding are

currently the subject of various research projects. For example, research is being conducted into the adhesive joining of a composite ship superstructure to the steel hull of a corvette and the use of thick-film bonding for deck superstructures [35,36]. In [2,16], it was demonstrated that structural steel bonded joints can also be used in direct contact with seawater. Furthermore, metal piping for shipbuilding can be economically manufactured using adhesive bonding under shipyard-specific conditions [37,38]. The bonding of brackets to primary marine structures can even be carried out underwater [39,40]. There are also numerous reports on the repair of ship structures using bonded reinforcement elements [41,42].

For adhesive joints in shipbuilding, additional requirements must be considered beyond mere force transmission. These include, amongst other things, high creep and temperature resistance, as well as good workability, particularly for thick-film bonding. Measurements taken on the deck of an ocean-going vessel show, for example, that adhesive joints there can be exposed to a temperature range of –30 °C to +70 °C [43]. In the case of direct contact with seawater, the temperature range is between 0 °C and +35 °C [31]. Many adhesive manufacturers now offer adhesive systems certified for maritime applications that meet the aforementioned requirements. Common systems used in the maritime sector include polyurethanes, epoxies and silicones. Acrylates are also used, for example in mountings, as they generally ensure rapid bond development [31].

1.3. Adhesive bonding of large structures in steel construction

For a long time, the bonding of large-scale, thick-walled steel components was considered unfeasible. However, it has increasingly become the focus of research in recent years. Various research projects in recent years have demonstrated that it is possible to bond large steel structures whilst achieving high joint load-bearing capacities and efficient assembly and fabrication processes. A key example (research project IGF No. 17199 N / P 884) focused on the development and systematic investigation of bonded joints between cast steel nodes and hollow steel sections for applications in structural steelwork [44,45]. As part of this project, suitable adhesives were selected and characterised to meet the specific requirements of structural steelwork. Following the development and validation of a manufacturing concept, the load-bearing capacity of the bonded cast steel-tube joint was tested, taking into account realistic imperfections, varying adhesive layer thicknesses, overlap lengths, tube diameters, different temperature conditions and after artificial ageing. The manufacture and quasi-static testing of sample components demonstrate that the bonded joint between a steel and a cast steel component can be produced with a consistently high load-bearing capacity.

Building on the positive results of these results, in [1,14] a bonded joint for legs and bracings for jacket structures in offshore wind turbines is developed. As part of extensive numerical and experimental investigations, a hybrid, bonded bracing connection was developed which exhibits a higher load-bearing capacity than the steel components to be connected, both under quasi-static and non-stationary loading conditions.

A further development of the joining process is the subject of [46], in which an innovative, hybrid joining process for steel components is investigated. The so-called hybrid adhesive-grout joining technique, which is particularly suitable for pipe-in-pipe pull-through joints, is characterised by a multi-layer structure combining inorganic and organic adhesive layers [46–49]. This results in a joint with very high performance, both under quasi-static and dynamic loading [50,51].

Additionally, Mantik et al. [52] investigated pre-stressed hybrid joints using closed-ring and blind rivet studs. The study showed that combining a riveted joint with an adhesive joint can achieve a significant increase in load-bearing capacity compared with riveted joints alone. In [53], Evers et al. are investigating the possibility of retrofitting weathered power-line structures hybrid-bonded bolted joints.

Another area of research in the field of adhesive technology is the refurbishment of structures using bonded CFRP laminates. In the construction industry, bonded CFRP laminates are currently used primarily for the retrofitting of reinforced concrete components. Kasper et al. [54–56] have conducted extensive research into the possibility of retrofitting fatigue-damaged steel structures using loose and prestressed bonded CFRP laminates. Their findings show a significant increase in residual service life compared with an unreinforced beam.

Based on the current state of research, recent research projects are increasingly focusing on the multifunctionality of adhesives. Adhesives based on epoxy resins and polyurethanes can be modified in such a way that, in addition to high strength, they also possess good damping properties. The viscoelastic behaviour of the adhesive results in material damping, which can contribute to structural damping. The damping properties of bonded joints are being comprehensively investigated in [57–59].

Recent studies on adhesively bonded hybrid structures show that the adhesive layer is increasingly used as a deliberate design element rather than merely a joining means. In aluminium/CFRP energy absorbers, bonding is employed to force a brittle composite to follow the deformation of a ductile metal frame, thereby guiding failure and stabilising progressive crushing [60,61]. Bashipour et al. [60] showed that the placement of the composite relative to the metal shell governs stability and specific energy absorption, and Ghasempoor et al. [62] demonstrated that local reinforcement of critical corner regions can retain most of the energy absorption of a fully wrapped section with a fraction of the composite material. Data-driven approaches have been added to predict the response of such bonded hybrids [62]. These studies address thin-walled aluminium/CFRP crash absorbers at small scale, where controlled failure of the bonded assembly is the desired outcome, and adhesive integrity is a stability condition under oblique loading [61,62]. For load-bearing stiffened steel plates in shipbuilding, the opposite objective applies: the bond line must transfer shear between profile and plate up to the plastic capacity of the profile without failure, on shipyard-supplied primed surfaces and at component scale.

To the authors' knowledge, systematic large-scale tests on adhesively bonded stiffeners under bending, including the influence of shop primer, are not available.

1.4. Scope of this Paper

This paper addresses the research gap identified in the previous section regarding the lack of systematic large-scale tests on adhesively bonded stiffeners under bending, including the influence of shop primer. It investigates adhesively bonded longitudinal stiffeners (IPE 80 and IPE 120) on 6 mm shop-primed AH36 deck plates, derived from the structure of a RoRo hoistable car deck. The novelty lies in (i) the component-scale bending tests with one and three stiffeners, (ii) the direct consideration of shipyard-supplied primed surfaces and their effect on bond performance, and (iii) the numerical derivation of the specimen from the full-scale structure. The objective is to determine whether the plastic bending capacity of the stiffeners can be utilised without bond failure, and under which surface preparation this holds. A key objective is to evaluate the feasibility of adhesive bonding for the attachment of stiffening elements in steel plate structures, taking into account industry-relevant requirements such as corrosion protection, manufacturing compatibility, and structural integrity. Both single-stiffener and multi-stiffener configurations are considered. The welded car deck structure used in practice serves as the reference for the numerical design of the bonded structure and the test specimens; the experimental programme itself focuses on the load-bearing behaviour of the bonded stiffeners and does not comprise parallel tests on welded specimens. Advantages of bonding over welding, such as reduced thermal distortion and preserved coatings, are therefore taken from the literature and are not quantified in this paper. The findings aim to provide technical foundations for the broader implementation of bonding processes in shipbuilding, including recommendations for surface pretreatment, adhesive selection, and process integration under shipyard conditions.

2. Materials and methods

2.1. Materials and samples

2.1.1. Adhesives

Two adhesive systems were selected for the present study based on previous investigations, in which they demonstrated excellent adhesion to the applied shop primer as well as favourable long-term durability under marine conditions. Accordingly, the two adhesive systems selected were the epoxy adhesive WEICON Easy-Mix HT 180 (WEICON GmbH & Co. KG, Germany) and the epoxy adhesive Fischer FIS EM Plus 390 S (fischerwerke GmbH & Co. KG, Germany). A comprehensive description of their selection and performance is provided in [63]. These durability data stem from coupon-scale tests reported in [63] and were used as a selection criterion for the adhesive systems investigated in the present study. Durability testing at the component scale addressed in this paper was outside the scope of the present investigation.

The selection process further considered the processing characteristics of the adhesives. In particular, an adequate pot life was essential, as the preparation and application of the large-scale specimens required an application time exceeding 15 minutes. Furthermore, two-component adhesive systems were chosen because they enable reliable curing over large bonded overlap areas without the need for external heat input, making them particularly suitable for large-scale structural bonding applications. In addition, both adhesive systems exhibit a non-sag, thixotropic consistency, allowing application not only on horizontal but also on inclined and vertical surfaces without adhesive flow or slumping.

The most important characteristics of the two prioritised adhesives are summarised in Table 1, based on [63,64]. The modulus of elasticity, Poisson's ratio and tensile strength were determined from tensile tests on bulk adhesive specimens in accordance with DIN EN ISO 527 [65]. The adhesive tensile strength on steel and on primer was determined from pull-off tests in accordance with ISO 4624 [66].

2.1.2. Primer

In shipbuilding, it is common practice to apply a shop primer to semi-finished steel products (sheets, sections, component segments) whilst they are still at the factory. Shop primers are temporary anti-corrosion coatings whose primary function is to protect materials and components from atmospheric corrosion during storage and manufacturing processes at the shipyard or on site. Consequently, semi-finished products are usually delivered to the shipyard already primed.

In industrial practice, shop primers are either overcoated during subsequent coating operations or locally removed prior to coating, depending on the specific manufacturing process and application requirements. Bonding directly to the shop primer offers significant

Table 1
Summary of the main characteristics of the two prioritised adhesives [63].

Composition	Weicon Easy-Mix HT 180 2-component epoxy resin adhesive, colour: black	Fischer FIS EM Plus 390 S 2-component epoxy resin adhesive, 30–40 % Portland cement, colour: grey
Pot life at room temperature	60 min	30 min
Modulus of elasticity	2,581 MPa	5,598 MPa
Tensile strength	27.0 MPa	45.0 MPa
Poisson's ratio	0.4	0.3
Adhesive tensile strength on steel surfaces	29.2 MPa	27.4 MPa
Adhesive tensile strength on PPG Sigmalweld 199 primer	16.7 MPa	13.3MPa

potential for reducing both manufacturing time and costs, as labor-intensive surface preparation steps, such as complete coating removal and abrasive blasting of the steel substrate, can be avoided. Consequently, the experimental investigations presented in this paper were performed on coated steel components. It should be noted that the primed steel plates investigated in the present study were obtained directly from shipyard operations and therefore exhibited partially surface contamination resulting from handling, storage, and transportation. Previous investigations identified wipe cleaning with isopropanol as the most practical and effective surface preparation method for such conditions (cf [63]). Consequently, the same cleaning procedure was adopted throughout the present study. The dry film thickness of the shop primer on the supplied plates was measured and is documented in [64]. The primer was applied following standard shipyard practice; the resulting variation in layer thickness was found not to affect the load-bearing capacity of the bonded stiffeners.

Bonding onto the shop primer is only viable if the primer itself provides sufficient adhesion to the substrate and to the adhesive. As this cannot be assumed for every supply batch, characterisation tests on the delivered primer are regarded as a prerequisite. If they fail, the primer has to be changed. Localised removal by sandblasting is possible but is not recommended in practice for cost reasons. (see section 2.3.2).

A comprehensive characterisation of two relevant shop primers is documented in [63]. Based on these investigations, the two-component zinc-(ethyl)silicate primer Sigmaweld 199 (PPG Industries) was selected for the subsequent test series, as it enabled the transfer of higher mechanical loads than the alternative primer system investigated. For Sigmaweld 199, the dry film thickness measured on the supplied plates averaged approximately 26 μm (range 20–28 μm), compared with a nominal value of 18 μm stated in the technical data sheet, and the pull-off adhesion strength [66] ranged between 13 and 19 MPa, consistent with the values reported in Table 1. Further details are documented in [63,64].

2.1.3. Steel materials

For the experimental investigations, IPE 80 and IPE 120 cross section types were used as longitudinal stiffeners. For tests involving a single stiffener section, a top plate section 300 mm wide was used at two different lengths (2 900 mm and 3 600 mm respectively). For tests on larger component groups with three stiffener elements arranged in parallel, plate sections with a width of 2,325 mm and a length of 3,600 mm were used. A thickness of 6.0 mm was specified for the deck plate arranged over the stiffeners, as representative of shipbuilding practice.

As IPE sections do not represent standard stiffener geometries used in shipbuilding and are commercially available in grade S355J2 (in accordance with DIN EN 10025-1 [67]), these profiles were used for the experimental programme and subsequently coated with the selected shop primer to ensure a surface condition representative of shipbuilding practice. A major reason for this is their low weight, their comparatively high rigidity and the available bonding surface.

However, the mechanical properties of S355 are considered equivalent to those of the shipbuilding steel grade AH36 (in accordance with ASTM A131) for the purposes of the present investigation. In contrast, the plate specimens were manufactured from AH36 steel, as this material is the standard plate material employed in shipbuilding and was obtained directly from shipyard operations, thereby ensuring representative boundary conditions with respect to the industrial manufacturing process.

Structural steel of grade S355 was nominally used as the material for all steel components employed. Nevertheless, the steel materials used for the component tests were supplied in separate batches and can be verified as not originating from the same production batch. To determine the mechanical and technological properties of the base material of the IPE sections used in the tests on specimens with one and three stiffener profiles, as well as of the cover plates, tensile specimens were prepared from the components and tested in a uniaxial tensile test in accordance with DIN EN ISO 6892-1 [68]. The tensile specimens from the web of the IPE 80

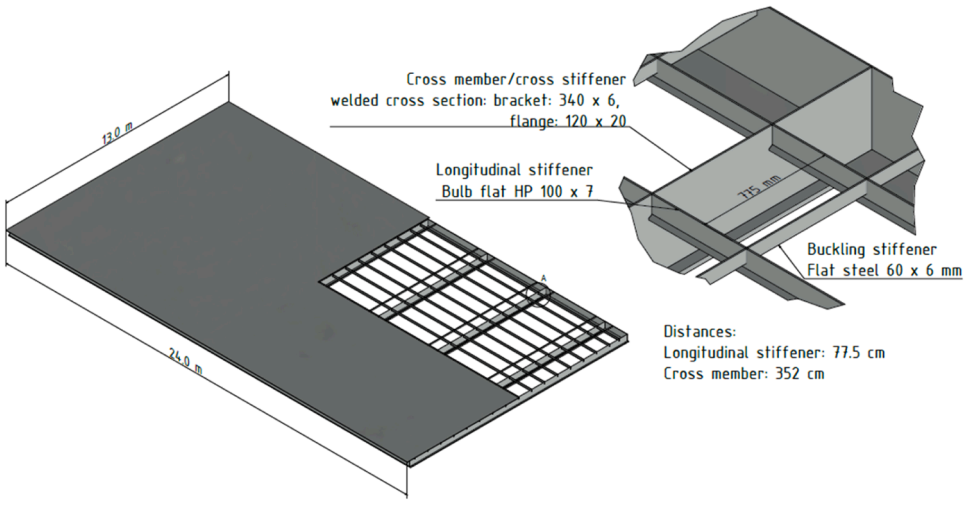


Fig. 1. Reference structure of a CarDeck of a reinforced in both the longitudinal and transverse directions, based on shipbuilding practice of RoRo ships.

profile were prepared as standard rectangular tensile specimens of type E in accordance with DIN 50125 [69]. The coating on the specimens was removed locally prior to the start of the test in order to determine the core sheet thickness, which was used as the basis for determining the material properties.

2.2. Development of the test specimens and the test setup

2.2.1. Reference structure from maritime practice

The test specimen was developed on the basis of the real geometry of a hoistable CarDeck, as is currently used in Roll on/roll of ships (RoRo ships), with welded stiffening profiles. The CarDeck under consideration is approximately 24 m long and 12 m wide. The load-bearing structure (girder grid), shown in Fig. 1, consists of cross-beams in the form of T-sections and longitudinal stiffeners connected to them on both sides, made from bulb flats HP 100 × 7 sections, each 3500 mm in length.

In addition, buckling stiffeners made of flat steel with dimensions of 60 × 6 mm are arranged in the longitudinal direction. The cross-members are positioned 352 cm apart, whilst the longitudinal stiffeners are spaced 77.5 cm apart. The CarDeck is enclosed on all sides by a perimeter frame made of T-sections. The application of adhesive bonding is of particular interest for such thin-walled structures, as conventional welding is known to induce significant welding distortions due to the local thermal input. These distortions often require extensive straightening and rework operations, increasing both production time and manufacturing costs. As a cold joining process, adhesive bonding largely avoids thermally induced distortions and therefore offers considerable potential for reducing post-processing efforts while improving dimensional accuracy. These advantages of a cold joining process are established in the literature (e.g., [70–72]) and they were not measured in the present study.

2.2.2. Numerical investigations into a test specimen with one and three stiffeners

2.2.2.1. Scope of the numerical investigations. The numerical model presented in this section serves two purposes only: to design a laboratory-scale test setup that reproduces the stress state of the steel components of the real CarDeck structure with sufficient accuracy, and to estimate the resulting stresses in the adhesive layer as a basis for adhesive selection. The model is not intended to predict failure of the bonded joint. A detailed, probabilistic treatment of adhesive bond failure, based on the material and specimen data of this study, is presented separately in [64]. A comparison between the numerical model and the experimental results is limited to the steel stress level used for the specimen design. A full comparison of force-displacement curves and strains between the design model and the tests is outside the scope of this design-oriented analysis.

2.2.2.2. Model development. To develop a laboratory-scale test specimen for the experimental investigation of adhesive-reinforced suspended deck structures, a CarDeck model based on a conventional shipyard design was first analysed numerically. To ensure that the experimental investigations were representative of practical applications, the deformations and stress distributions of the industrial CarDeck structure were analysed numerically. Based on these results, the test specimen was designed to reproduce deformation characteristics and load transfer mechanisms comparable to those of the full-scale structure under representative loading conditions. Conventional shipbuilding structures typically employ HP (bulb flat) sections, which consist of a flat steel section with an integrated bulb and are fillet-welded directly to the deck plate. While this geometry is well suited for welded joints, it is not compatible with structural adhesive bonding, as the profile provides only a very limited bonding surface, preventing the formation of an adequately sized bonded overlap. Consequently, the stiffener geometry had to be modified to achieve a bond-line configuration suitable for adhesive joining. For the HP profiles commonly used in shipbuilding, this was accomplished by welding an additional flat steel plate to the profile, thereby creating a sufficiently large bonding surface. As an alternative approach, commercially available standard IPE steel sections with different cross-sections were investigated as a more economical solution, as their flange geometry inherently provides a large bonding area while offering structural behaviour comparable to the modified HP profiles. Fig. 2 illustrates the development of the stiffener concept from the conventional welded HP profile to the adhesive-compatible design concepts investigated in the present study.

2.2.2.3. Material models and properties used for numerical analysis. Steel and the adhesive were modelled as linearly elastic materials, as the expected deformations under representative service loads remain within the elastic range. Moreover, structural adhesive

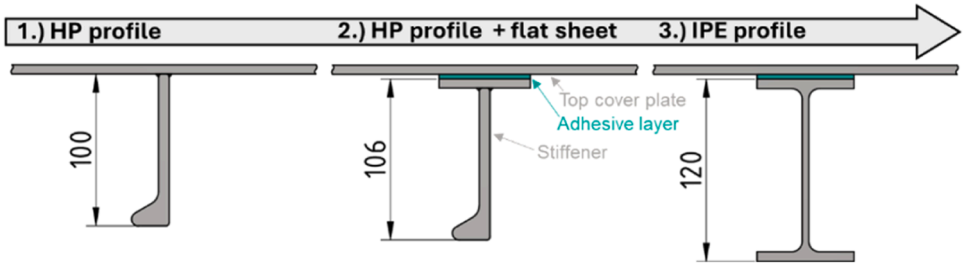


Fig. 2. Adaptation for adhesive bonding of structures reinforced with conventional, welded HP profiles.

systems exhibit an approximately linear elastic response at the low strain levels considered. The material parameters documented in Table 2 are used, whereby a representative, fictitious adhesive with a realistic modulus of elasticity of 1000 MPa is modelled.

2.2.2.4. Calculation model of the CarDeck. In the context of the numerical analyses, the focus was on the adhesive bonding of the longitudinal stiffening profiles. The CarDeck is modelled in ANSYS Workbench 2023 R2 as a quarter-model, utilising the two existing axes of symmetry. The 3D-element types SOLID186 and SOLID 187 were used to model the bodies as continuum elements. In the actual structure, the CarDeck is supported at six discrete points, where it is suspended by tension rods within the vessel, allowing its height to be adjusted according to the cargo configuration. The model is supported at the four edge points and at the centre along the long side. Deformations are restrained in all axial directions. Rotation is permitted freely in all axial directions.

The starting point is the conventional welded car deck with bulb flat HP stiffeners, as used in practice. Based on this design, a bonded variant was defined in which the HP stiffeners are modified to provide a sufficiently large bonding surface (Fig. 2). The deformation and stress states in the steel components of the bonded global model were compared with those of the welded construction. This comparison serves two purposes: it shows that replacing the welded joints by bonded joints does not change the load-bearing behaviour of the deck in the range relevant for design, and it provides the reference values (deformation, stresses in the steel and in the adhesive layer) on which the design of the test specimen and the test setup are based. Both global and local deformations and the stresses in the adhesive layers and steel components were determined under a representative surface load, including a dynamic surcharge of 3.5 kN/m^2, based on [73,74].

2.2.2.5. Numerical model of the experimental setup. The geometry and configuration of the test specimens were derived from the numerical analyses of the full-scale bonded deck. The aim is to reproduce the deformation and stress states of the reference (bonded global model) in the steel components and in the adhesive layer as accurately as possible in a laboratory-scale specimen. In this way, the load-bearing behaviour of a representative cover plate section with bonded stiffeners can be studied in a four-point bending test and related to the behaviour of the full-scale structure. The numerical model thus provides the basis for the design of the specimen and the test rig; it is not intended to compare bonded and welded joints.

Based on the design of the reference component, the test specimen is, in principle, constructed from a longitudinal stiffening profile and an overlying top cover plate section, between which a 6 mm thick adhesive layer was applied. A bond line thickness of 6 mm was selected, since the large spans encountered in ship structures may be subject to considerable tolerances, potentially resulting in wide gaps that must be bridged. This value therefore represents a conservative estimate. The selection of stiffening profiles suitable for adhesive bonding was carried out following an analysis of conventional steel structural profiles, particularly with regard to the weight-to-stiffness ratio. For the experimental investigations, the IPE 80 and IPE 120 sections were selected.

In the numerical model, the test specimen is rigidly connected on both sides to two cross-member sections. In this way, the welded joints that occur in practice between the longitudinal and cross-members, as well as between the top plate and the cross-members, are realistically simulated.

The model of the test specimen with one longitudinal stiffener is shown on the left in Fig. 3; the cross-section is shown on the right. The adhesive layer is meshed in the thickness direction using three elements. The support of the test specimen is implemented in the model via body supports at the cross-beam sections. To determine the steel stresses, two defined deformation boundary conditions are applied at the one-third points, which corresponds to a four-point bending test. The required deformation boundary conditions are determined on the basis of the effective deflection of a reference section of the global model, thereby ensuring that the results are comparable.

The test specimen with three stiffening elements is defined on the basis of the analysis results for the test specimen with one stiffening element. The structural configuration is retained. As an extension, three stiffening elements are positioned side by side at a defined spacing of 775 mm. The top plate and support profiles are enlarged accordingly. The selected longitudinal stiffener spacing is taken from the CarDeck model.

It was found that the connection detail between the cross-beams and longitudinal beams is a key parameter governing the stress concentrations at the edges of the adhesive joint. Based on this finding and considering manufacturing-related aspects, two connection variants were investigated numerically and experimentally. On the one hand, a hinged bolted connection with a welded flange plate. On the other hand, a flexurally rigid ‘end-plate joint’, in which end plates welded on both sides are connected by bolts. This paper presents exclusively the results of the tests involving the end-plate joint. The results of tests carried out on samples with flange plates are documented in [64]. The use of a bolted plate-to-plate connection allows the support profiles to be reused, thereby reducing manufacturing effort and material consumption.

Table 2
Parameters of the materials used in the numerical calculations.

	Steel	Adhesive
Density [kg/m^3]	7,850	-
Poisson's ratio [-]	0.3	0.45
Modulus of elasticity [MPa]	210,000	1,000
Shear modulus [MPa]	81,000	345

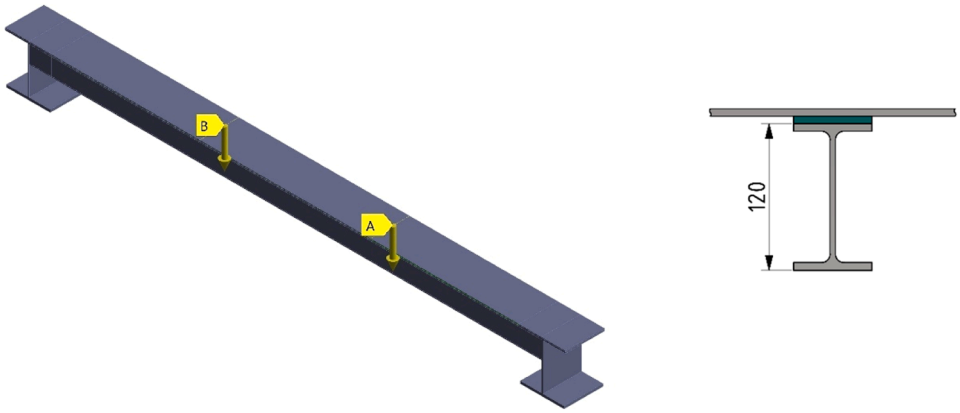


Fig. 3. Left: Numerical calculation model of the test specimen; right: cross-section of the test specimen, showing an example with an IPE 120 stiffener profile.

2.3. Manufacture of test specimens

As a basis for the production of test specimens, a process-integrated adhesive application method, including fixing devices, was first developed and tested. In addition, combined surface pretreatment methods for different substrates (with/without shop primer) were defined and evaluated, and the manufacturing concept was implemented and validated in practice using a demonstrator. In addition, specific cleaning and application protocols were established, and prioritised pretreatment methods were defined for each adhesive system.

The following section first describes the process for manufacturing test specimens with a single stiffening element. Building on this, Section 2.3.2 deals with the extension of the process to the manufacture of test specimens with three stiffening elements.

2.3.1. Test specimen with one stiffener

For the practical manufacturing process, precise cleaning protocols were first established. Coarse contaminants on the primed components were removed mechanically by sweeping and scraping with soft wooden spatulas. This was followed by degreasing with technically pure ethanol, followed by a final degreasing with pure isopropanol. These cleaning cycles were repeated at least twice.

In the second production step, the adhesive was applied to the cover plate. A specific device was developed for this purpose, the front end of which consists of a head plate with two triangular cut-outs of different sizes. The resulting triangular adhesive fillet represents a common joint design feature intended to prevent air entrapment during assembly. By rotating the plate, the carriage can be adjusted to produce test specimens with IPE 80 or IPE 120 stiffener profiles. The cross-section of the adhesive bead was optimised for each stiffener profile in preliminary tests to ensure that the applied adhesive volume resulted in only minimal squeeze-out after assembly, thereby avoiding any post-processing.

As shown in Fig. 4, the adhesive is injected directly into the carriage. Once the carriage has been sufficiently filled, it is pulled over the cover plate.

The two adhesive components are extruded through a static mixer using a cartridge press to ensure they are mixed in accordance with the manufacturer's specifications. Depending on the cartridge size, it may be necessary to change cartridges several times. Fig. 4 shows, on the right, the slide being withdrawn and the resulting triangular bead of adhesive. This approach enabled a straightforward and reproducible adhesive application under laboratory conditions. Although the procedure was performed manually in the present study, semi-automated dispensing systems capable of handling comparable adhesive volumes are already available and could be



Fig. 4. Left: applying the adhesive to the reservoir of the applicator; Right: Moving the applicator and forming a triangular bead of adhesive.

adapted for shipbuilding applications.

The components are joined by positioning the IPE section (prepared with spacers) centrally on top of the cover plate coated with adhesive. The thickness of the adhesive joint is of crucial importance here. To achieve a defined adhesive layer thickness, spacers are clamped between the flanges of the IPE section (Fig. 5). Once in place, the stiffening profile is secured over the spacers using clamps. The tightening torque is low, as only the position of the beam needs to be secured, and no contact pressure is required. Deformation of the cover plate must be avoided. Instead, any geometric tolerances are compensated for by the adhesive layer, thereby preventing elastic preloading of the steel components and the generation of residual stresses within the adhesive. The clamps are removed once the adhesive has fully cured.

Once the adhesive has fully cured, the final production step involves welding end plates to both sides, each 140 mm high, 120 mm wide and 12 mm thick. The MIG welding process is used for this. First, the end plates are aligned and tacked to the web of the IPE beam with four tack welds each in welding process step 1. The lower flange is then welded to the end plate using a fillet weld (step 2). Finally, the end plate is joined to the top plate by a high-temperature weld (step 3, Fig. 6).

The a-dimension is set to 3 mm to minimise heat input. The welding operations are also monitored using a thermal imaging camera, which records the temperature in the joint area throughout the entire welding process at four measurement points over a length of 50 mm, starting from the end of the stiffener profile. It was confirmed that the temperatures in steps 1 and 2 do not exceed 160°C and, in particular, decrease rapidly after step 1. The results indicate that no thermally induced damage occurred within the adhesive layer, and that the bond integrity was therefore not compromised by the welding heat input.

2.3.2. Further development of the manufacturing and assembly concept to produce test specimens with three stiffening elements

The production of the test specimens with three stiffening elements was adapted to suit the dimensions of the cover plate section.

Prior to the cleaning stage, the primer coating in the bond area was removed by mobile sandblasting (cleanliness grade Sa 2½) on two of the three large-scale specimens (V3-F-IPE80-B and V2-W-IPE120-B); the third specimen (V2-F-IPE80-P) was bonded on the as-supplied primer and serves as a reference for the effect of primer quality.

This deviation from the concept of bonding directly onto the shop primer was not a design choice but a consequence of a manufacturing issue: tensile adhesion tests (results documented in [64]) showed that the primer on the plates supplied for the three-stiffener series had markedly lower adhesion than the primer on the plates used for the single-stiffener specimens (Section 2.3.1). The primer properties therefore differed between supply batches, which illustrates that variation in primer quality must be expected in industrial supply chains. Since the primer quality of the single-stiffener series had already been shown to be sufficient, replacing the plates was considered neither necessary for the research question nor justifiable in terms of material and priming costs and sustainability. Instead, blasting was applied so that the large-scale bending tests could be carried out and the question of whether several bonded stiffeners can reach the plastic capacity of the profiles could be answered independently of the primer issue. The three-stiffener results with blasted surfaces therefore demonstrate the capacity of the bonded joint, but they do not demonstrate bonding directly on the primer at component scale.

The subsequent cleaning was carried out in the same way as the process described in Section 2.3.1. The holes in the cover plate required for bolting were drilled using a magnetic drill before the test began. To do this, the three stiffener profiles were first lifted into place, aligned and bolted to the end plates (Fig. 7, left), the end plates having already been welded to the stiffener profiles on both sides prior to the start of production. The cover plate was then lifted into position once and aligned; the required holes were marked out using a template and drilled to a diameter of 18 mm. Once all the holes had been drilled, the cover plate was lifted out again (Fig. 7, right). To ensure a defined adhesive layer thickness, the spacers familiar from section 2.3.1 were used; these are clamped between the flanges of the IPE sections, with at least five equidistantly spaced spacers.

Due to a sufficiently long pot life and a high extrusion speed of the Fischer FIS EM Plus adhesive, all three stiffeners could be bonded in a single operation. After applying the adhesive to all the stiffeners, the cover plate was lifted into place and bolted to the HEM profiles through the pre-drilled holes. As the bolts were tightened immediately whilst the adhesive was still uncured, no internal stresses were introduced into the subsequent bonded layer.

When using the Weicon Easy-Mix HT 180 adhesive, the three stiffeners were bonded sequentially due to the small container size and a lower extrusion speed. After applying the adhesive to one stiffener, the cover plate was lifted into place and bolted to the HEM



Fig. 5. Test specimen with one stiffening profile bonded to the centre of the top cover plate after the adhesive bonding process.

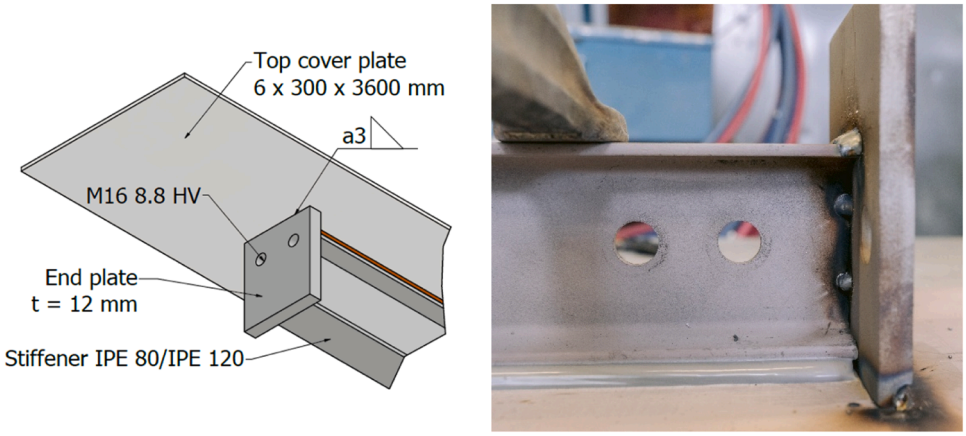


Fig. 6. Test specimen with a stiffening profile bonded centrally following the adhesive bonding process.

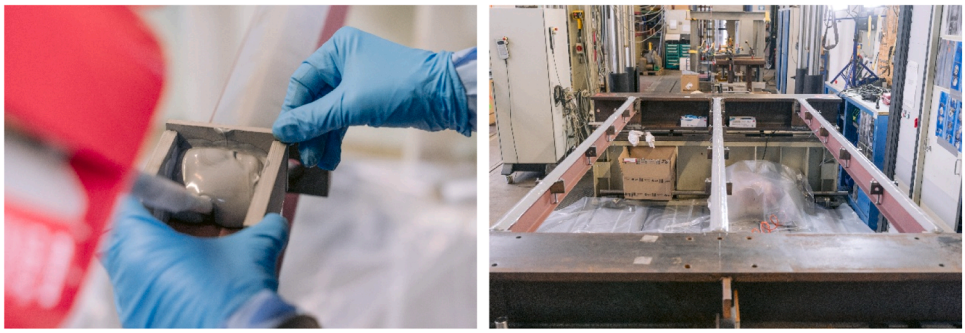


Fig. 7. Left: Adhesive being applied to a stiffener element of the components with three stiffeners; Right: Adhesive application completed, prior to lifting into place and joining the cover plate.

profiles. After a curing time of at least 24 hours, the screw connections were loosened and the cover plate was lifted out to allow for a further application of adhesive. The profile that had already been bonded was secured in the centre of the sheet metal panel using a bracket assembly made of hollow sections and threaded rods, in order to prevent damage to the bond. This procedure was repeated twice. Once all the stiffening profiles had been bonded, the connections between the end plates and the top plate were finally established. To this end, four spot welds were carried out through holes previously drilled in the top plate, connecting the upper surfaces of the end plates to the top plate (see Fig. 8).

2.4. Experimental investigations into plate elements stiffened by one adhesively bonded stiffening element

2.4.1. Test setup

The test setup for the four-point bending tests carried out is shown schematically in Fig. 9. The test specimen, consisting of a top

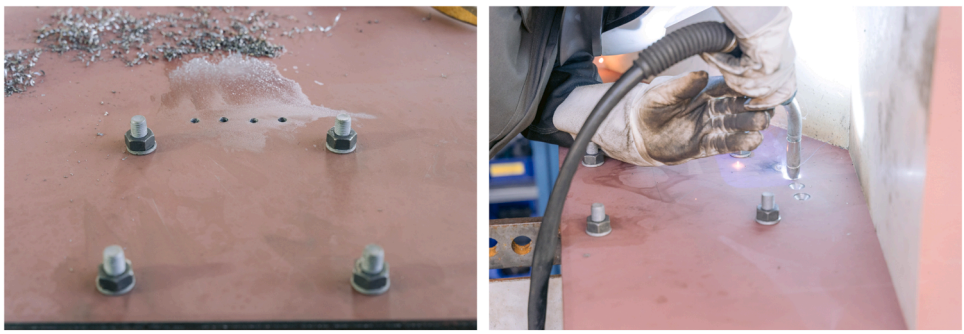


Fig. 8. Close-up of the bolted joint on the cover plate (left) and the spot welds used to join the end plates and the cover plate (right).

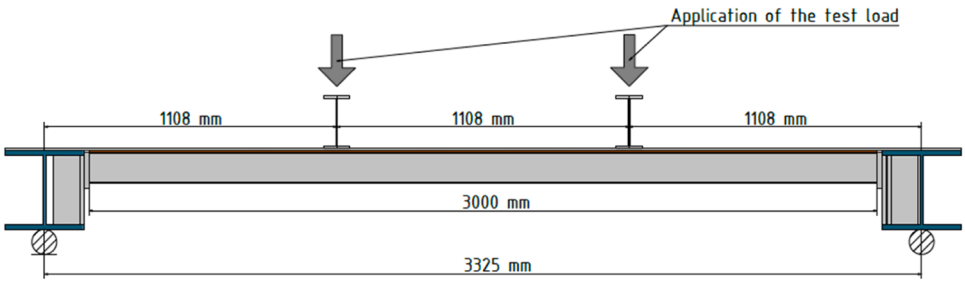


Fig. 9. Schematic illustration of the four-point bending test on plate elements stiffened by adhesive bonding using a stiffening element.

cover plate and a stiffening profile bonded to it, is connected on both sides to HEM300 profiles using bolts via end plates. The HEM sections represent the transverse stiffeners present in the car deck, between which the longitudinal stiffeners are mounted.

The bolting connection in the area of the end plates between the HEM section and the stiffener section is secured on both sides using two pre-tensioned M18 8.8 HV bolts on each side. In addition, the cover plate is bolted to the HEM profile on both sides using five M18 8.8 HV bolts on each side. The applied preload, together with the high coefficient of friction between the components, prevents relative displacement between them. This replicates, in a test setting, the welded joint between the longitudinal and transverse stiffeners that exists in practice.

In addition to machine force and machine displacement, local deformations and local strains of the components are recorded using additional measuring equipment. Three displacement transducers and three strain gauges were used to analyse the tests. The positioning of the measuring instruments is shown in Fig. 10. The displacement transducers located below the load application point and the displacement transducer in the centre of the span enable the local bending stiffness of the test specimens in this area to be calculated as part of the test evaluation. The strain gauges at the three positions shown allow, in particular, an analysis of the normal bending stresses across the cross-section height, which enables, amongst other things, an assessment of the bond and the attainment of the plastic load-bearing capacity of the IPE section.

In Fig. 11 the actual test setup is shown in a side view and a top view. In addition, Fig. 11 shows detailed photographs of the support area and the end plate connection.

The tests were carried out under controlled and constant ambient conditions at a test speed of 3 mm/min. The load is released as planned in the event of specimen failure or once the HEM profile comes to rest on the support blocks as a result of rotation. The machine force and displacement, as well as the readings from the displacement transducers and strain gauges, are recorded and documented.

2.4.2. Test program

The tests documented in Table 3 were carried out.

In these tests, the adhesive, the type and the length of the stiffener profile were varied. Due to the very low variation in the relevant range of the curve for the analysis as well as the very high manufacturing effort per test specimen, only two tests were carried out for each test configuration. This paper discusses the influence of the stiffener length, using adhesive Weicon Easy-Mix HT 180 as an example.

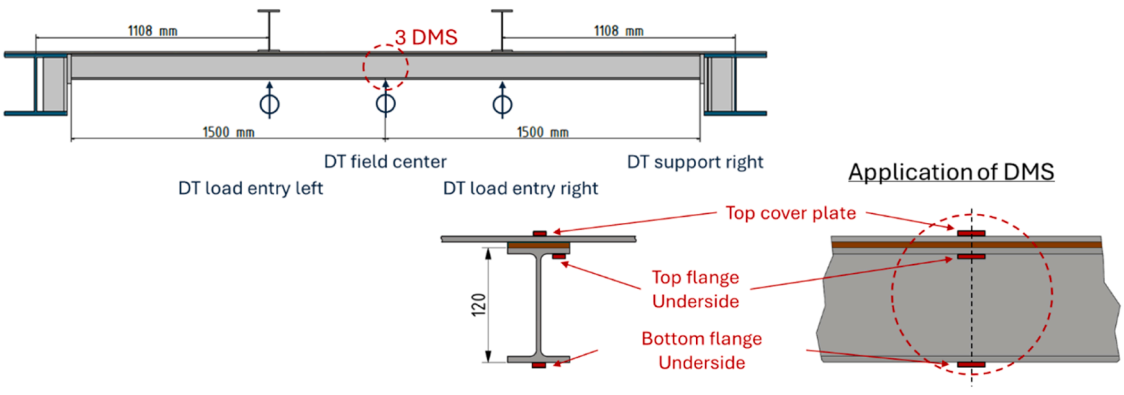


Fig. 10. Positioning of displacement transducers and strain gauges on the test specimen.

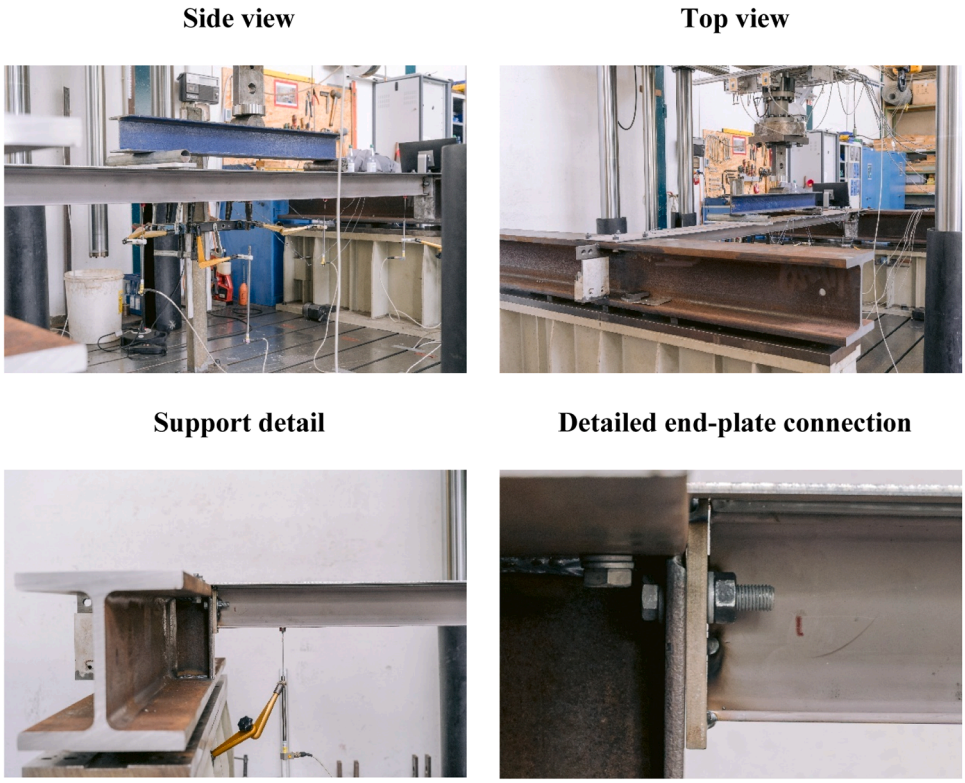


Fig. 11. Set-up of the test in the testing machine (views and detailed images).

Table 3
Test matrix for four-point bending tests on panel components stiffened by adhesive bonding with one stiffening element.

Length stiffener	Adhesive	Stiffener type	Tests
3000 mm	Fischer FIS EM 390 S	IPE 80	2
		IPE 120	2
	Weicon Easy-Mix HT 180	IPE 80	2
		IPE 120	2
2500 mm	Weicon Easy-Mix HT 180	IPE 80	2
		IPE 120	2

2.5. Experimental investigations into plate elements stiffened by three adhesively bonded stiffening elements

2.5.1. Test setup

Large-scale component tests were carried out to investigate the load-bearing behaviour of flat plates stiffened by adhesive bonding in dimensions relevant to practical applications. The test specimens used for this purpose were based on the single specimens with a single stiffening element described previously. To extend the scope of the investigation, three stiffening elements with a length of 3000 mm were applied in parallel in the longitudinal direction in order to evaluate the interaction between multiple stiffening elements and their influence on the overall load-bearing behaviour. Fig. 12

The tests were carried out as four-point bending tests. The test setup essentially corresponds to that used for bending tests on test specimens with a single stiffening element (see Section 2.4.1, Fig. 9). To accommodate the greater width, the load-application IPE 200 profiles were extended across the entire width of the top cover plate.

The bolting connection in the area of the end plates between the HEM section and the stiffener section is secured on both sides using two pre-tensioned M18 8.8 HV bolts on each side. In addition, the cover plate is bolted to the HEM profile on both sides using five M18 8.8 HV bolts on each side. The applied preload, together with the high coefficient of friction between the components, prevents relative displacement between them. This replicates, in a test setting, the welded joint between the longitudinal and transverse stiffeners that exists in practice.

In addition to machine force and machine displacement, local deformations and local strains of the components are recorded using additional measuring equipment. Nine displacement transducers are used per test. The position of the displacement transducers is

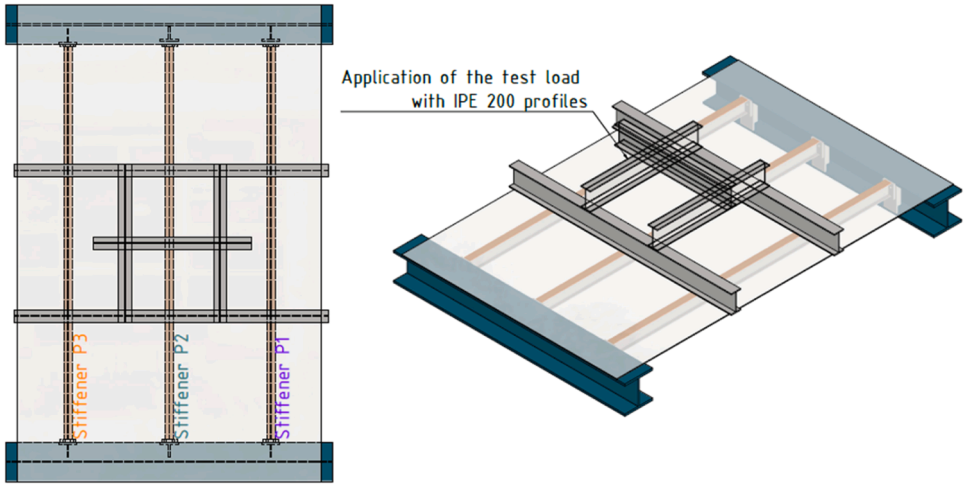


Fig. 12. Top view and isometric view of the four-point bending test on plate elements stiffened by adhesive bonding using three stiffening elements.

determined in the same way as in the tests carried out on test specimens using a stiffening element (see Fig. 10). In addition, strain gauges are applied to the three stiffener profiles and the top plate. The arrangement of the strain gauges in the area of the stiffeners is the same as in the tests carried out on specimens with a single stiffener (see Fig. 10). Furthermore, strain gauges are positioned on the upper surface of the top cover plate in the centre of the field, midway between the stiffeners. In total, five strain gauges are positioned on the top plate.

The tests were carried out under controlled conditions at a test speed of 3 mm/min. The load is released as planned in the event of specimen failure or once the HEM profile comes to rest on the support blocks as a result of rotation. The machine force and displacement, as well as the readings from the displacement transducers and strain gauges, are recorded and documented.

2.5.2. Test program

Based on the preceding investigations, selected tests were conducted on large-scale specimens featuring three stiffening elements. Because the primer on the supplied plates showed reduced adhesion (2.3.2), one test was carried out on the as-supplied primed surface (V2-F-IPE80-P) to document the effect of primer quality, and two tests were carried out on surfaces from which the primer had been removed by sandblasting (index B) to determine the capacity of the bonded joint independent of the primer: V3-F-IPE80-B (Fischer FIS EM 390 S, index F) and V2-W-IPE120-B (Weicon Easy-Mix HT 180, index W). Owing to the size and manufacturing effort of the three-stiffener specimens, each of the three configurations (V2-F-IPE80-P, V3-F-IPE80-B, V2-W-IPE120-B) was tested once. The results for these configurations therefore represent single observations, without a statistical measure of scatter; the reproducibility established for the corresponding single-stiffener configurations (section 3.3) is used as supporting evidence that the observed behaviour is representative.

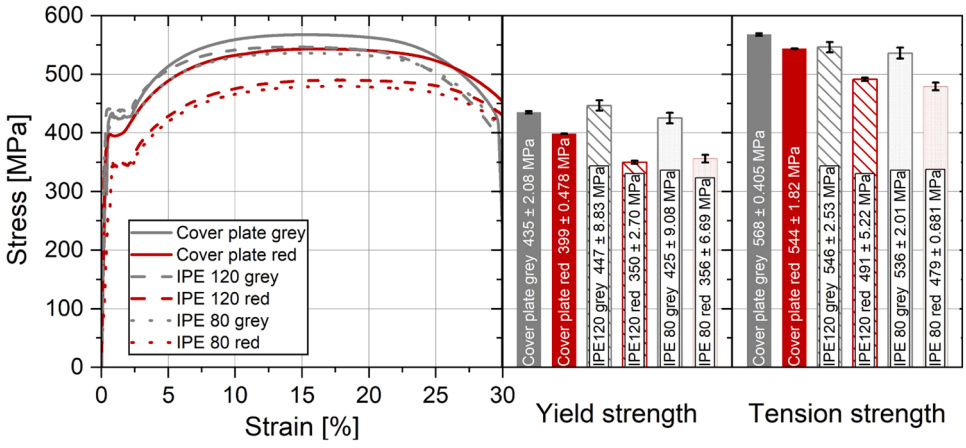


Fig. 13. Results of tensile tests on tensile specimens made from the steel components.

3. Results

3.1. Material characterisation

3.1.1. Steel properties

The results of the mechanical and technological property determination carried out on the material of the steel components used are shown in Fig. 13. The Fig. shows the curves in the stress-strain diagram, as well as the yield strengths and tensile strengths derived from them. The results for the tests using a single stiffener are shown and coated with shop-primer in grey. In contrast, the results for the tests using three stiffeners are shown and coated with shop-primer in red.

The measured yield strengths range on average between 356 MPa and 447 MPa. It can be observed that the components coated with red primer exhibit yield strengths that are 8 to 22 % lower than those of the components coated with grey primer. This difference is not caused by the primer: it reflects a difference in the base material strength between the steel supply batches used, one of which happened to be coated with red primer and the other with grey primer at the supplier. The primer colour therefore serves only as an identifier of the supply batch in this context and has no influence on the steel strength. In particular, the stiffener profiles primed with red primer exhibit significantly reduced yield strengths. The tensile strengths follow the same trend: the components primed with red primer exhibit tensile strengths that are 4 to 11 % lower than those of their grey-primed counterparts. The measured tensile strengths range on average between 479 MPa and 568 MPa. Specific numerical averages for each component are documented in Fig. 13. The results of the characterisation of the mechanical and technological properties of the steel components are primarily used to evaluate the results of the bending tests carried out on stiffened plate components in section 3.3 and 3.4. The focus here is on achieving the plastic load-bearing capacity reserves of the stiffening profiles during the course of the tests.

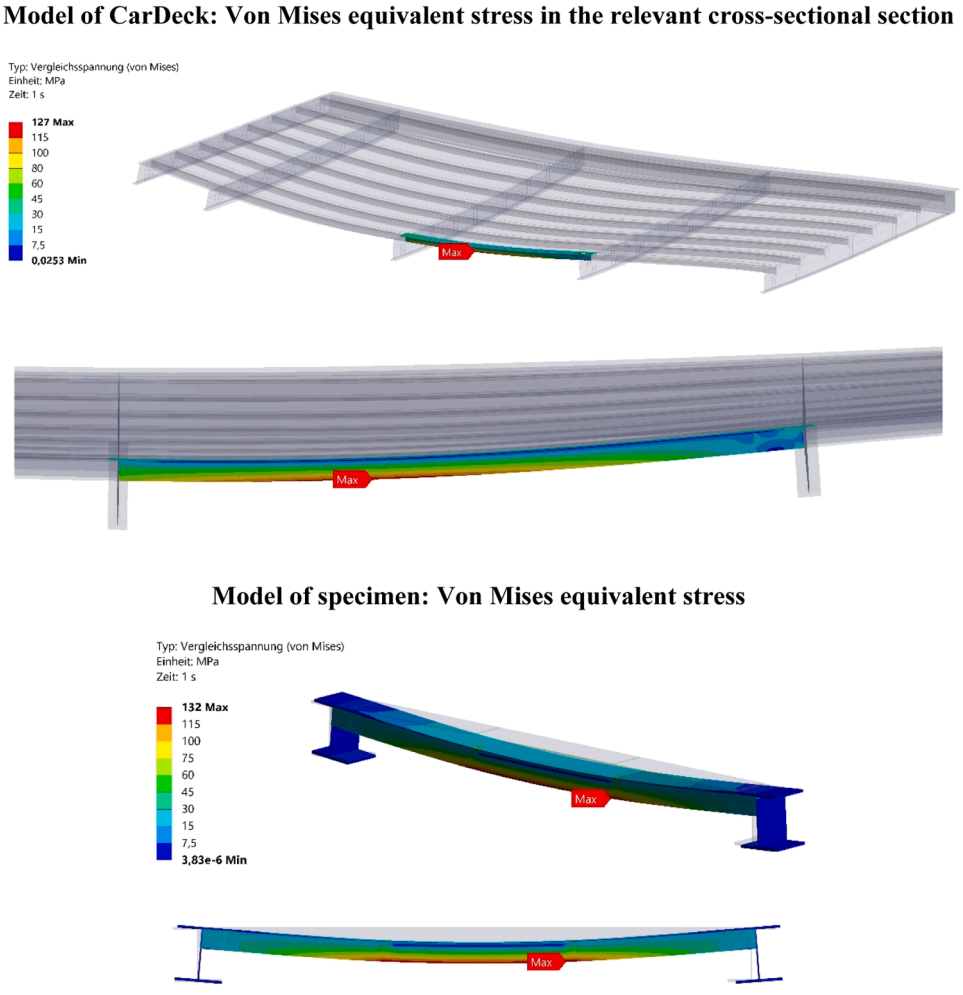


Fig. 14. Comparison of the von mises equivalent stress in the relevant cross-sectional section of the CarDeck model and in the test specimen.

3.2. Design of the test specimen based on the global model

For the subsequent analyses, the effective deflection was defined as the difference between the deformation of the critical longitudinal stiffener and that of the adjacent cross-girders; this effective deformation lies in the range of 7.0–8.0 mm. The maximum von Mises equivalent stress in the longitudinal girder was 127 MPa, occurring in the flexural tensile zone, and served as the basis for the specimen design. For a stiffener length of 2500 mm, the deformation ratio between the global model and the specimen corresponds to an equivalent deformation of 5.4 mm applied at the third-point locations.

A comparison between the global car deck model and the test specimen (Fig. 14) shows good qualitative and quantitative agreement in the von Mises equivalent stress, particularly at mid-span: 127 MPa (global model) versus 140 MPa (specimen, 2500 mm) and 127 MPa versus 132 MPa for the extended 3000 mm specimen [64]. This is a design comparison at the level of steel stresses and does not constitute a validation of the model against test results.

Normal and shear stresses in the adhesive layer along a defined analysis path were likewise compared between the global model and the specimen (Fig. 15). Normal stresses remain generally below 0.5 MPa, with locally increased compressive stress beneath the load-application line; shear stresses remain below 2.0 MPa in both cases, well within the non-critical range for the adhesive layer.

In summary, the four-point bending setup reproduces the deformation and stress state of the global model closely, particularly for the longer stiffener length, supporting the extrapolation of the experimental results to the bonded CarDeck structure. This specimen design was retained and extended for the three-stiffener tests: three stiffening profiles at 775 mm centre-to-centre spacing beneath a 2400 × 3600 mm top cover plate (Fig. 16), mirrored along the longitudinal axis, so that the previously established stress and strain states were expected to recur for each stiffener.

3.3. Bending behaviour of adhesively stiffened panel components with one stiffening element

Unless noted otherwise, the force–deflection curves of all single-stiffener tests follow the same pattern: an initial linear rise, followed by a flattening of the slope once the underside of the IPE profile begins to yield, and a further, markedly reduced slope until the test is terminated due to excessive rotation of the HEM support profiles.

For the 3000 mm specimens (Fig. 17), the linear range ends at 20–25 kN for the IPE 80 profile and 50–55 kN for the IPE 120 profile; maximum test loads of 25–27 kN (IPE 80) and 64–67 kN (IPE 120) were reached. The strain-gauge evaluation (Fig. 18) confirms this mechanism: the transition from the linear to the flattened branch coincides with the onset of yielding on the tension side (24 kN for IPE 80, 52.3 kN for IPE 120). Looking at Fig. 18, at 0.21 % strain, assuming E = 210,000 MPa, the corresponding stress of 441 MPa agrees with the tensile test results on the steel components (Section 3.1.1). Strains on the top cover plate remain compressive and linear until the profile yields, with no change in slope that would indicate loss of bond.

For the 2500 mm specimens with Weicon Easy-Mix HT 180 (Fig. 19), the linear range ends at 30 kN (IPE 80) and 65 kN (IPE 120), with maximum loads of 34 kN and 67 kN, respectively, which is consistent with the behaviour described above.

Two deviations from this general pattern were observed. Specimen V1-IPE80 exhibited localised pre-existing damage (65 cm, at the side of the IPE profile near the right-hand support) prior to testing, caused by the brittleness of the adhesive during handling. The test was nevertheless carried out to assess the residual load-bearing behaviour. Failure occurred abruptly at 22.2 kN (top plate buckling), with the load dropping to 13.3 kN and subsequently recovering to 18.1 kN at reduced stiffness. Specimen V2-IPE80 had to be discontinued prematurely due to failure of the end-plate welds, unrelated to the bonded joint; up to that point, its initial stiffness matched the other specimens and the recorded section is included in Fig. 19.

3.4. Bending behaviour of adhesively stiffened panel components with three stiffening elements

3.4.1. Test V2-F-IPE80-P

Fig. 20 shows the deformation at the centre of the field of the three stiffeners as a function of the machine force for test specimens

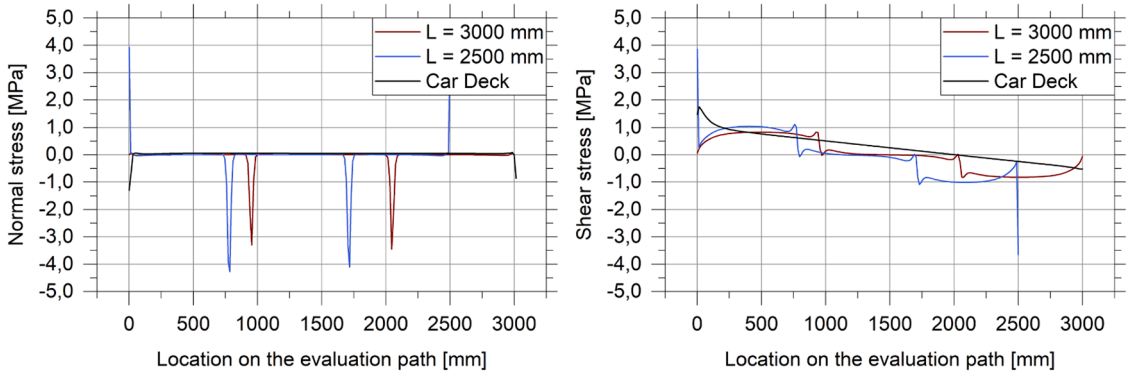


Fig. 15. Normal and shear stress in the longitudinal direction of the bonded layer along the evaluation path at the centre of the bonded layer.

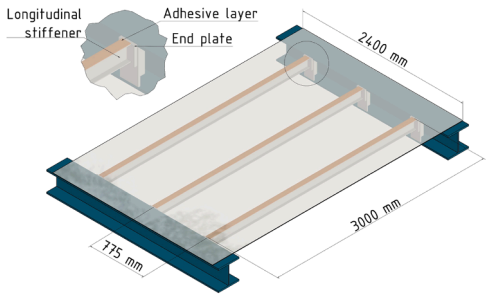


Fig. 16. Test specimen with three stiffening elements.

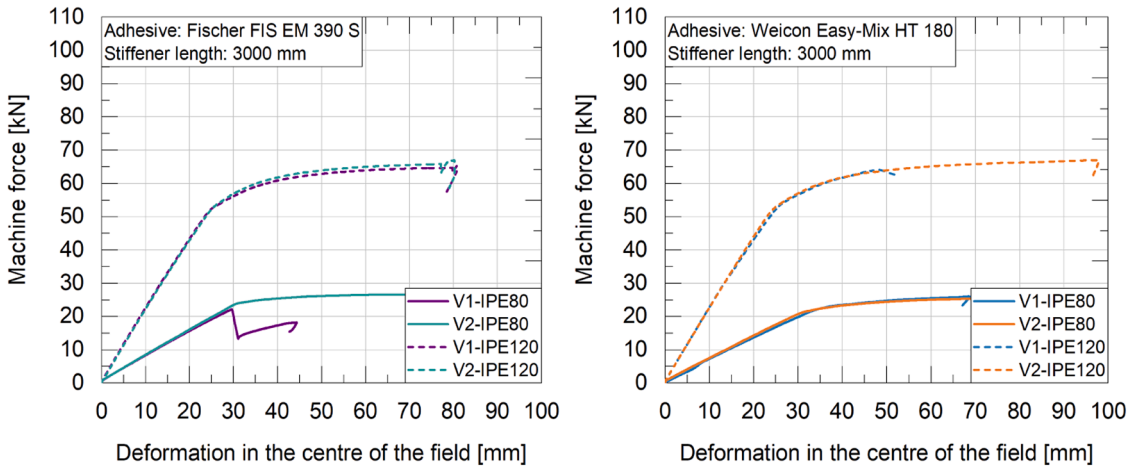


Fig. 17. Diagram showing deformation in the centre of the field as a function of machine force for test specimens with a stiffener length of 3000 mm and stiffener profiles IPE 80 (solid lines) and IPE 120 (dashed lines) for the two adhesives Fischer FIS EM 390 S (left) and Weicon Easy-Mix HT 180 (right).

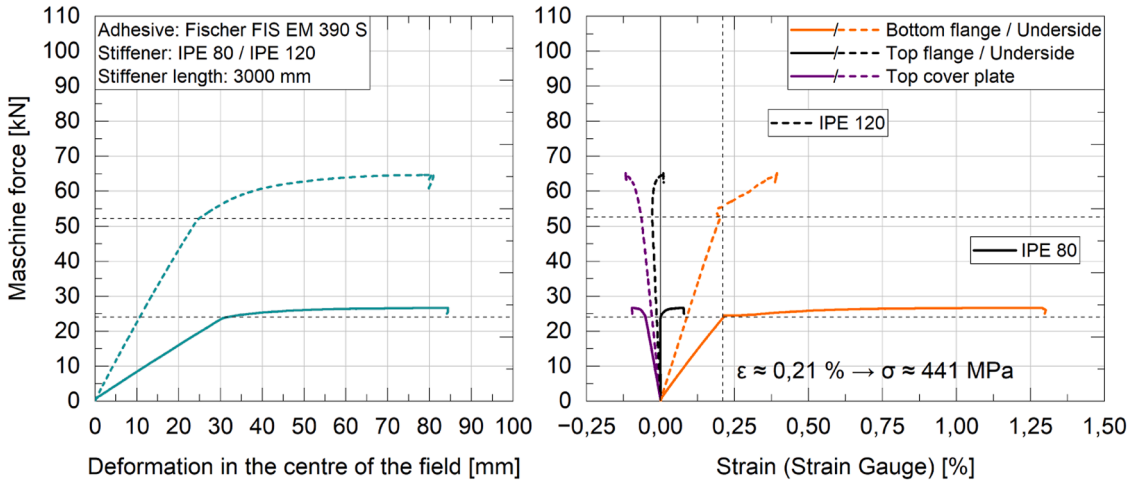


Fig. 18. Exemplary evaluation of the recorded strains based on the three strain gauges applied to the test specimens, for one test specimen each with an IPE 80 and an IPE 120 profile; adhesive: Fischer FIS EM 390 S.

with an IPE 80 stiffener profile. The specimen is manufactured with the adhesive Fischer FIS EM 390 S and with primered components.

The force-deformation diagram initially shows a linear rise in the curves for all three stiffeners. At a machine force of approximately 10 kN, an initial slight drop in the load can be observed. The partial failure of stiffener 1 was clearly detected acoustically, as an audible

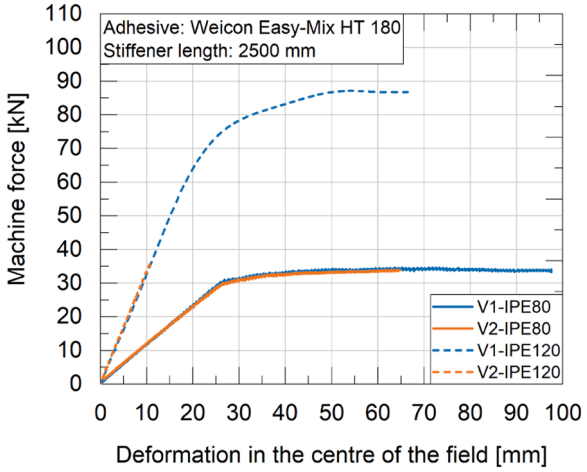


Fig. 19. Diagram showing deformation in the centre of the field as a function of machine force for test specimens with a stiffener length of 2500 mm and stiffener profiles IPE 80 (solid lines) and IPE 120 (dashed lines) by way of example, as a representative selection for the adhesive Weicon Easy-Mix HT 180.

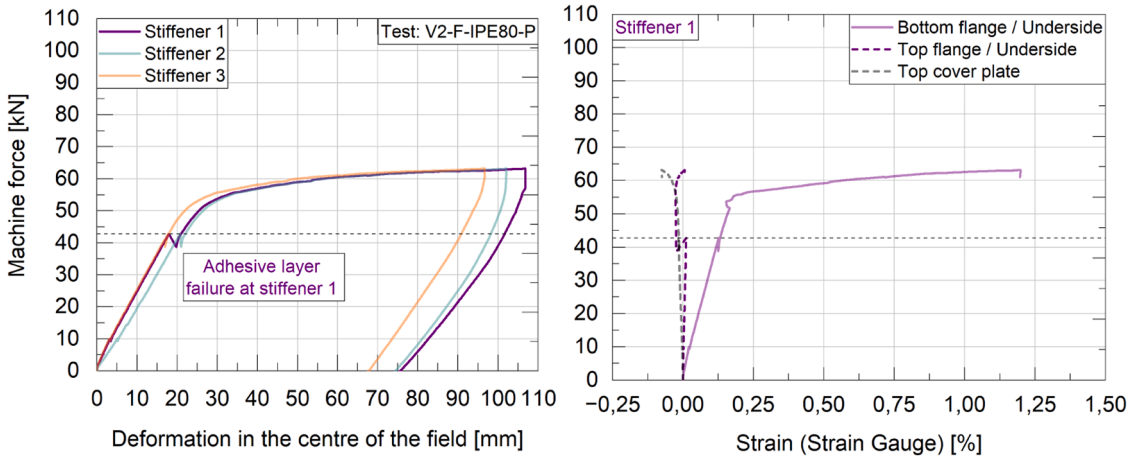


Fig. 20. Left: Deformation of the three stiffeners in the centre of the field as a function of machine force in test V2-F-IPE80-primered; right: exemplary evaluation of the recorded strains based on three strain gauges applied to the underside of the bottom flange of stiffener 1 and on the top cover plate directly above stiffener 1.

cracking sound, and was visually observable as a local opening of the bond line in the support region. Because the failure was located in the support region rather than in the middle of the specimen, its effect on the mid-span displacement measurement was limited, and the corresponding load drop in Fig. 20 is only slightly pronounced.

At a load of approximately 42 kN, a progression of the adhesion failure for stiffener 1 and a significant drop of the corresponding load curve can be observed. Thereafter, the slope of the test curves decreases continuously up to a force of 62 kN. The test curves then run approximately horizontally until the test is terminated at approximately 63 kN.

On the right side of the diagram in Fig. 20, the strains recorded using strain gauges at three measurement points across the cross-section for the test specimen are analysed. These strain curves initially show a linear trend, analogous to the force-deformation curves. At a machine force of approximately 42 kN, a drop in load and a sudden change in the recorded strains can be observed. Of particular interest here is the strain on the underside of the upper flange, which is shown as the purple curve in the diagram.

The curve initially shows positive strains, and the cross-sectional section is under tension. At the point where the load drops, the curve jumps into the region of negative strains (compression), from which a shift in the zero-stress line can be deduced. This change in the zero-stress line may be attributed to the failure of the adhesive bond. From this point onwards, there is no longer a composite cross-section, and the two cross-sectional parts bear the load as individual components over a large part of the span length. The yield limit on the underside of the stiffener profiles is therefore reached significantly earlier than expected and is consequently of no interest for further analysis.

Based on the low adhesion of the primer supplied for these components ([64]) and the resulting partial bond failure in test V2-F-

IPE80-P, the bonding surfaces of the following specimens were sandblasted (Sa 2½) prior to bonding. The aim was to reach the yield limit of the stiffener profiles in the large-scale component tests without failure of the adhesive bond.

3.4.2. Test V3-F-IPE80-B

The curves for all three stiffeners in Fig. 21 rise linearly. The slope decreases continuously from approx. 49 kN to approx. 63 kN and then continues with a gentle slope until termination at approx. 65 kN, with no indication of bond failure. Stiffener 2 deforms slightly more than stiffeners 1 and 3 up to approx. 10 kN, attributable to component tolerances giving it marginally higher initial stiffness. Beyond this load, the three stiffeners share the load evenly. The strain evaluation confirms the absence of local failure: strains in the top cover plate remain linear throughout, while strains on the profile underside increase disproportionately from 49.8–51 kN, marking the onset of yielding at approx. 0.16 % strain (approx. 330 MPa), consistent with the yield strength determined for the red-primed IPE 80 sections (Section 3.1.1).

Strain gauges on the top cover plate (Fig. 22) show markedly higher strains directly above the stiffeners than midway between them, indicating shear lag: load is introduced predominantly through the stiffener flanges, so the effective width of plate contributing to the composite bending stiffness is smaller than the 775 mm stiffener spacing. This is consistent with classical effective-width concepts for stiffened plates and is not specific to adhesive bonding; a quantitative derivation of the effective width from the present data was outside the scope of this study. Overall, V3-F-IPE80-B shows that a reliable bond can be maintained with multiple stiffeners up to the plastic capacity of the profiles, provided the bonding surface (blasted or adhesion-verified primer) offers sufficient adhesion, as the contrast with V2-F-IPE80-P illustrates.

3.4.3. Test V2-W-IPE120-B

The curves of test V2-W-IPE120-B in Fig. 23 rise linearly, with the slope decreasing continuously between approx. 125 kN and approx.150 kN and then continuing gently until termination at approx. 159 kN. No bond failure was observed. The disproportionate strain increase on the profile underside from approx. 125 kN (approx. 0.16 %, approx. 334 MPa) marks the onset of yielding, while strains on the cover plate remain compressive and linear throughout, confirming that the composite cross-section remained intact for the full test duration. After testing, all three stiffeners remained firmly bonded to the cover plate (Fig. 24), confirming that, with this adhesive and an adequately adherent primer or blasted surface, a reliable bond can likewise be maintained up to the plastic capacity of the IPE 120 profiles with multiple stiffeners.

4. Discussion

As part of the discussion of the test results, the influence of adhesive type, stiffener profile and field or stiffener length is systematically investigated. All diagrams in this section show the mean value and the standard deviation of the local bending stiffness across the repeated tests of each configuration, allowing the scatter of the results to be assessed directly. The results from test specimens with a stiffener profile length of 3000 mm serve as examples for a detailed examination of the influence of the adhesive and stiffener profile. The analysis is based on the evaluation of the local bending stiffness in the region between the load application point and the centre of the field. For this purpose, those sections of the load-deflection curves are considered which lie within the force range of 2 kN to 18 kN (IPE 80) or 2 kN to 45 kN (IPE 120), and in which the behaviour of the test specimens is approximately linear.

Local bending stiffness is used as the key parameter for the discussion, as it is largely independent of external influences, such as those from the support area. In this way, comparability of the individual test specimens can be ensured on the basis of a parameter

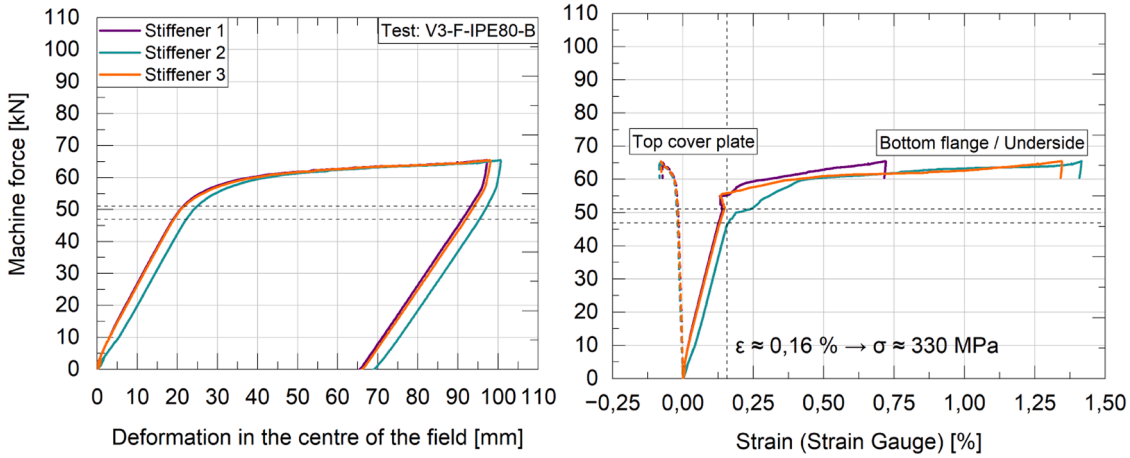


Fig. 21. Left: Deformation of the three stiffeners in the centre of the field as a function of machine force in test V3-F-IPE80-B; right: exemplary evaluation of the recorded strains based on three strain gauges applied to the underside of the bottom flange of stiffener 1 to 3 and on the top cover plate directly above stiffeners 1 to 3.

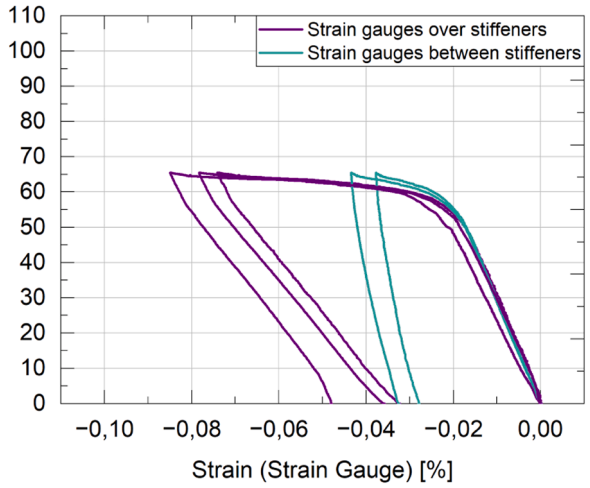


Fig. 22. Exemplary evaluation of the recorded strains based on five strain gauges applied to the upper side of top cover (purple: strain gauges directly over the stiffeners, green: Strain gauges between the stiffeners).

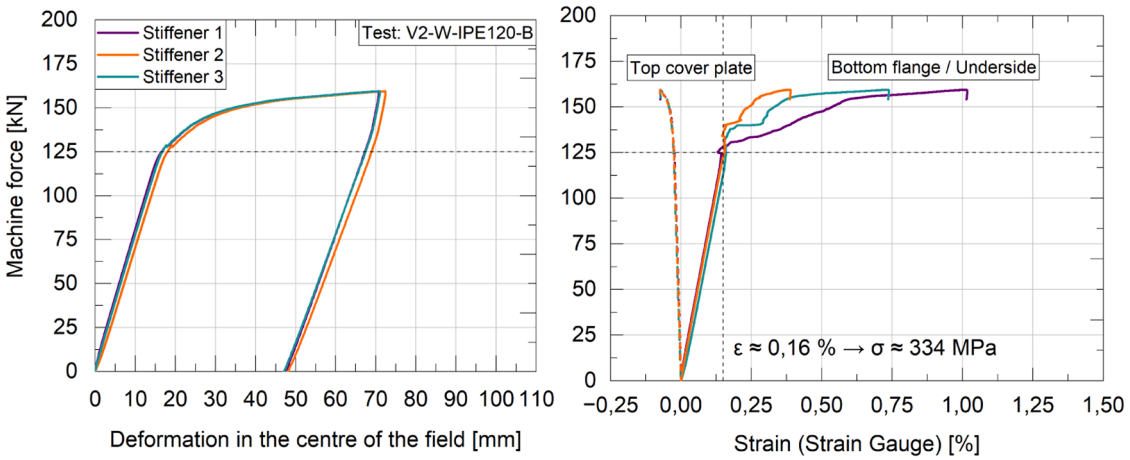


Fig. 23. Left: deformation of the three stiffeners in the centre of the field as a function of machine force in test V2-W-IPE120-B; right: exemplary evaluation of the recorded strains based on three strain gauges applied to the underside of the bottom flange of stiffener 1 to 3 and on the top cover plate directly above stiffeners 1 to 3.

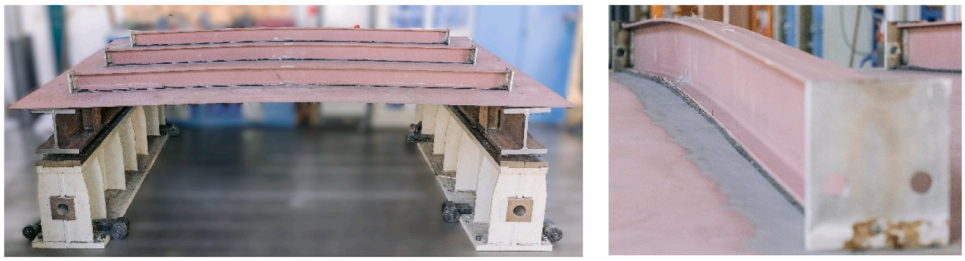


Fig. 24. Plastic deformation of the stiffeners after the end of test V2-W-IPE120-B (test specimen removed from the test setup and turned upside down).

relevant to components subjected to bending stress.

The local bending stiffness within the specified range is calculated in accordance with DIN EN 408 [75] using the following equation:

$$E_{m,I} = \frac{a l_1{}^2 \times (F_1 - F_2)}{16 \times (w_1 - w_2)} \quad (1)$$

With: a: Distance between a load point and the nearest support in a bending test [mm]
l_1: Measurement length for determining the modulus of elasticity
$(F_1 - F_2)$: Load increment in the selected range [N]
$(w_1 - w_2)$: corresponding deformation increment [mm]

Although DIN EN 408 originates from structural timber testing, Eq. 1 does not contain any material-specific assumptions: it is the classical mechanics-based relation for determining the apparent bending stiffness of a beam from the force and deflection increments measured in a symmetric four-point bending test, derived from beam theory. The equation is therefore equally applicable to steel–adhesive composite sections.

Across all tests reported in this study, only two cases of (partial) failure related to the bonded assembly were observed, and both had an identifiable, avoidable cause outside the adhesive bond itself. In test V1-IPE80, pre-existing local damage occurred during placement of the specimen in the test rig, prior to loading, as a result of the high brittleness of the adhesive (section 3.3). This is a handling issue rather than a consequence of the load-bearing behaviour of the bonded joint. In test V2-F-IPE80-P, partial adhesion failure occurred under load because the primer on the supplied plates did not provide sufficient adhesion (section 3.4.1, section 2.3.2). In test V3-F-IPE80-B and V2-W-IPE120-B, where the joint surfaces were sandblasted, no failure of the bonded joint occurred up to the plastic capacity of the stiffener profiles. This is consistent with the comparatively low stresses in the adhesive layer that result once the specimen and the bond area are dimensioned appropriately, as also indicated by the numerical stress analysis (section 2.2). Adhesive bond failure was therefore never observed as a consequence of the bond itself being overstressed; the two occurrences resulted from insufficient adhesion of the underlying primer and from handling damage prior to testing, respectively. In shipbuilding practice, such causes can be avoided by verifying primer adhesion before bonding (section 2.1) and by appropriate handling procedures for large bonded panels, particularly before the adhesive has reached its final strength.

4.1. Influence of the adhesive

Figs. 25 and 26 each summarise all the test results on the left-hand side. Fig. 25 shows the results for test specimens with an IPE 80 profile, whilst Fig. 26 documents the results for test specimens with an IPE 120 profile.

For the test specimens with the IPE 80 profile, the mean local flexural stiffness is 47.1×10^{10} Nmm^2 when using the Weicon adhesive Easy-Mix HT 180 and 44.9×10^{10} Nmm^2 when using the Fischer adhesive FIS EM 390 S. The mean standard deviation of the results is very low at 0.9×10^{10} Nmm^2. It can be seen that the mean value of the local flexural stiffness of the test specimens produced with adhesive Weicon Easy-Mix HT 180 is slightly higher than that of the test specimens produced with Fischer FIS EM 390 S. However, this can be explained by the small number of tests. Taking into account the standard deviation mentioned, no significant influence of the adhesive on the local flexural stiffness can be detected here either.

The mean local flexural stiffness of the test specimens with an IPE 120 profile is 136.7×10^{10} Nmm^2 for the adhesive Fischer FIS EM 390 S adhesive and 145.5×10^{10} Nmm^2 for adhesive Weicon Easy-Mix HT 180. The mean standard deviation of the measured values is 6.3×10^{10} Nmm^2, which is slightly higher than that of the test specimens with an IPE 80 profile. Here, too, it can be seen that the mean value of the local flexural stiffness of the test specimens produced with Weicon Easy-Mix HT 180 is slightly higher than that of the test specimens produced with Fischer FIS EM 390 S.

In both s, the analytically calculated values for the local flexural stiffness are also shown. The analytical bending stiffness assumes full bonding between the two components. For the purposes of simplification, an adhesive layer has not been taken into account. It can be seen that the experimental results can be well approximated by the analytical calculations. Overall, it can be concluded that the influence of the adhesive used on the local flexural stiffness of panel components reinforced by adhesive bonding is minor.

However, practical construction constraints must also be taken into account when evaluating the results. As the modulus of elasticity of the adhesive increases, the stress peaks in the adhesive layer also increase. This can have a negative impact on the load-bearing capacity of the bonded joint. Furthermore, as the modulus of elasticity increases, the practical suitability decreases, as the bond's robustness against manufacturing-related tolerances diminishes. These aspects must be taken into account, particularly with regard to manufacturing conditions in shipyards.

4.2. Influence of the stiffener profile

To analyse the influence of the stiffener profile on local bending stiffness, Fig. 27 (left-hand side) shows, by way of example, one test result each for the adhesives Fischer FIS EM 390 S and Weicon Easy-Mix HT 180, as well as for the two stiffener profiles IPE 80 and IPE 120, in the machine force-deformation in the centre of the field diagram. In addition, the result of the analytical calculation in the region of linear elasticity is shown for each case. On the right-hand side of the figure, the mean local bending stiffnesses determined both analytically and experimentally are plotted separately for each test combination.

The analysis shows that changing the stiffener profile from IPE 80 to IPE 120 results in an increase in the local bending stiffness of the test specimens by more than a factor of three. However, it can be seen that this marked difference in bending stiffness between the IPE profiles is not transferred to the same extent to the local bending stiffness of the entire composite cross-section. This means that, whilst the improvement in stiffness with increasing profile size is significant, it is not fully realised in the composite with the facing sheet and the adhesive layer.

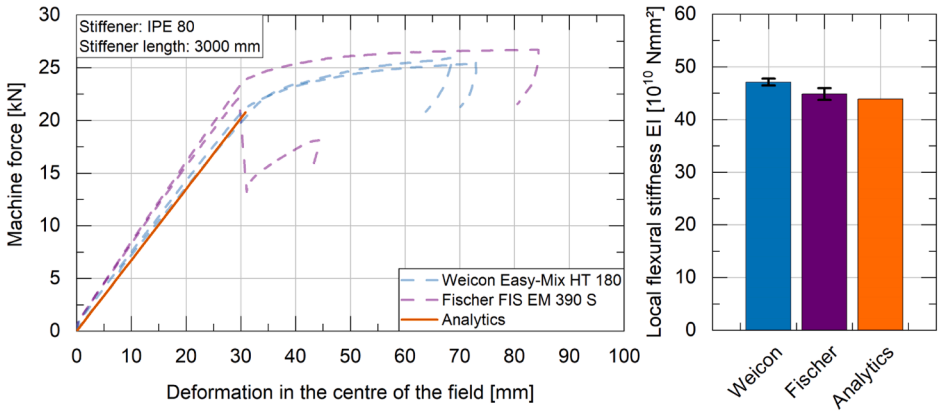


Fig. 25. Analysis of the analytically determined and experimentally measured local flexural stiffness of test specimens with an IPE 80 profile, based on the machine force-deformation curves at the centre of the field for the two adhesives, Fischer FIS EM 390 S and Weicon Easy-Mix HT 180.

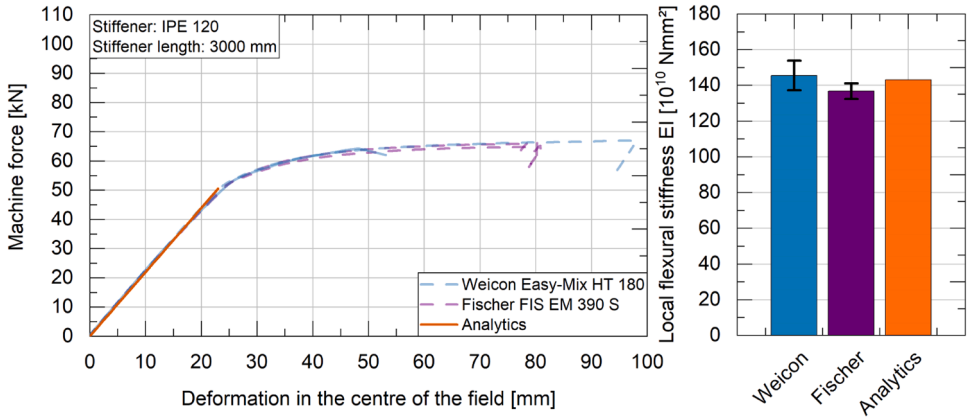


Fig. 26. Analysis of the analytically determined and experimentally measured local flexural stiffness of test specimens with an IPE 120 profile, based on the machine force-deformation curves at the centre of the field for the two adhesives, Fischer FIS EM 390 S and Weicon Easy-Mix HT 180.

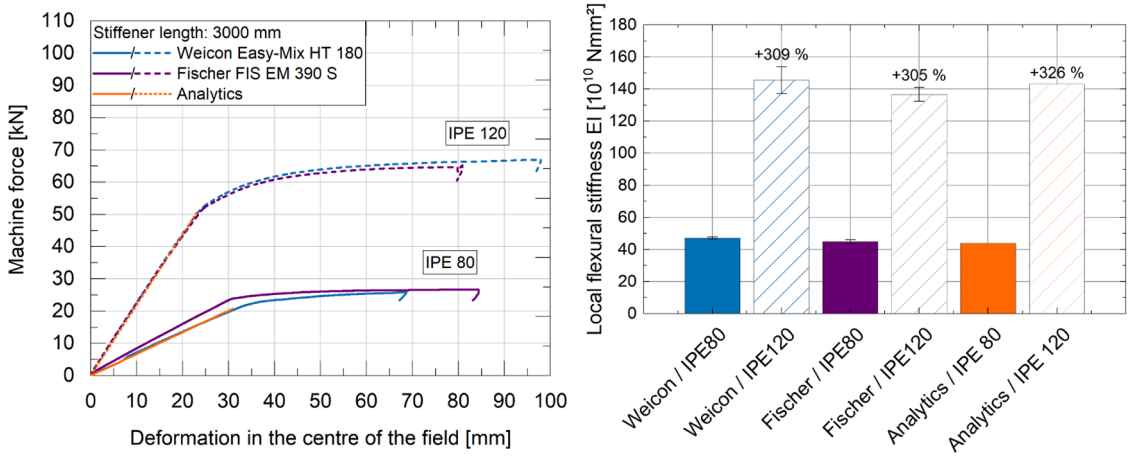


Fig. 27. Comparison of the analytically determined and experimentally measured local flexural stiffness of test specimens with IPE 80 and IPE 120 profiles, based on the force-deflection curves at the centre of the specimen for the two adhesives, Fischer FIS EM 390 S and Weicon Easy-Mix HT 180.

In addition to local bending stiffness, the chosen stiffener profile has a significant impact on the weight of the overall structure. The following considerations assume full bonding between the components and a constant number of longitudinal beams.

At 10.4 kg/m, the IPE 120 section has a significantly higher weight than the IPE 80 section, which weighs 6.0 kg/m. An increased section weight leads to greater deflections due to the dead load, as well as to higher steel consumption. Thus, the approximately threefold increase in local bending stiffness achieved by using the IPE 120 section is offset by a 1.7-fold increase in section weight and, consequently, a correspondingly higher material requirement.

These section-specific considerations can be applied to the scale of real structural members. With regard to the overall load-bearing behaviour, it can be seen that the maximum deflections of the global model can be varied by approximately ±10 % compared with the welded base model, depending on the stiffening profile used. This comparison is purely numerical and refers to stiffness only. Strength, fatigue and residual stresses of welded and bonded variants were not compared.

A reduction in maximum deflection by 11 %, on the other hand, requires a 39 % increase in the amount of steel used in the longitudinal beams. In relation to the entire model, the use of IPE 120 sections results in an increase in the structure's weight of approximately 9 %.

In summary, it can be stated that an increase in the moment of inertia of the stiffener profile leads to an increase in the bending stiffness of both the composite cross-section and the overall system. However, this is accompanied by an increase in dead weight, the quantity of steel required and the associated material costs. However, it was demonstrated that full bonding of the components could be achieved for both stiffener profiles. The choice of stiffening profile can therefore be made taking into account all the constraints relevant to the practical execution (weight, stiffness, cost).

It should be noted here that all of these considerations are based throughout on a 6 mm cover plate, as derived from the welded construction. In the adhesive-bonded variants, however, it would be possible to reduce the cover plate thickness, which would in turn yield a more favourable weight ratio.

4.3. *Influence of the stiffener length*

Based on the previous analyses, the question arises as to what extent the experimental results obtained can be extrapolated to real structures with varying stiffener lengths. Fig. 28 shows one representative experimental result for each combination of profile length and adhesive tested, using test specimens with the IPE 80 profile and IPE 120 profile, as well as the evaluation of the mean local bending stiffness of all tests, broken down by profile length for the Weicon Easy-Mix HT 180 adhesive.

It can be seen that, as expected, the global stiffness of the test specimens decreases as the profile length increases. The reason for this is the increasing influence of the specimen's connection in the support area on its global stiffness and the fact that the stiffener length is included in the calculation of the local bending stiffness as a square term according to Eq. 1. However, only a minor influence of the profile length on the local bending stiffness of the test specimens can be observed. For the IPE 80 stiffener profile, the local bending stiffness is approximately constant. For the IPE 120 profile, a slight increase in local bending stiffness of 9.2% can be observed as a result of increasing the stiffener length from 2500 mm to 3000 mm.

4.4. *Comparison of the load-bearing behaviour of stiffened panel components with one and three stiffeners*

To analyse the influence of the number of stiffeners on the general load-bearing behaviour of components stiffened by adhesive bonding, the results of tests on large components with three stiffener elements are compared with the results of tests on components with a single stiffener profile, the stiffeners having a length of 3000 mm. The general load-bearing behaviour of the test specimens and

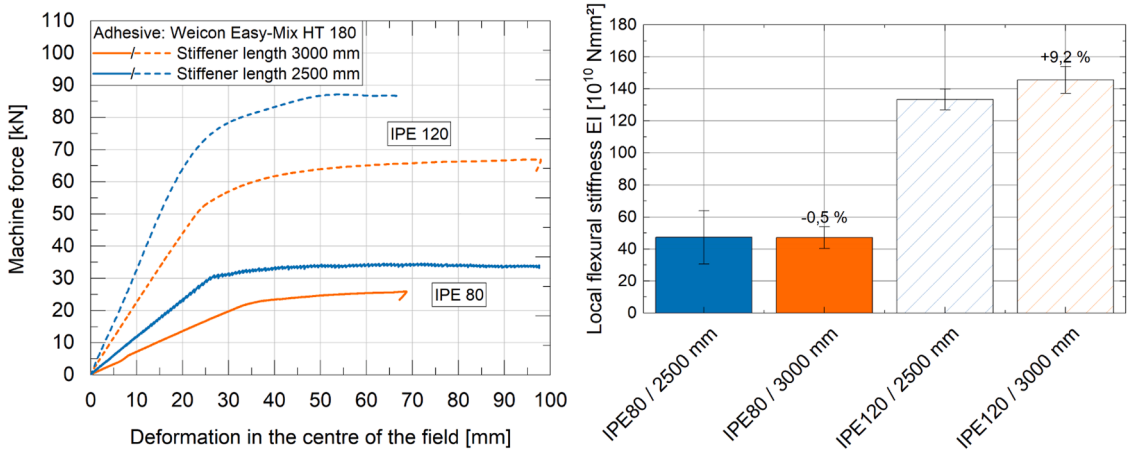


Fig. 28. Presentation of a representative test result for each combination of profile length and adhesive tested on test specimens with an IPE 120 profile, and evaluation of the local flexural stiffness of all tests, separated by profile length, for the Weicon Easy-Mix adhesive.

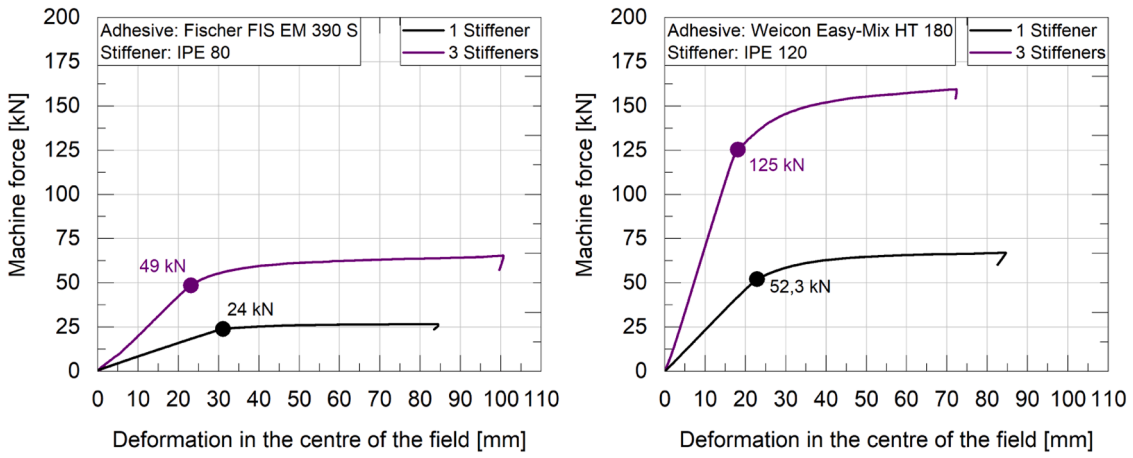


Fig. 29. Comparison of the load-deformation behaviour of test specimens with one and three stiffening elements, shown in a machine force–deformation in the centre of the field diagram for the two profile types IPE 80 and IPE 120.

the machine forces at the point at which elastic load-bearing behaviour ceases serve as a particular reference here.

In Fig. 29 an illustrative comparison of the load-deformation behaviour of the test specimens with one and three stiffener is shown for the two profile types IPE 80 and IPE 120. To illustrate the test curves for the test specimens with three stiffening elements, tests V3-F-IPE80-B and V2-W-IPE120-B, with blasted joint surfaces, have been selected.

In addition, Table 4 provides a comparison of the evaluated global and local stiffnesses of the test specimens with one and three stiffening elements, as a function of the stiffening profile. This table also records the machine forces at the point at which the elastic behaviour ceases (exceeding the yield strength). Here, the test specimens with the IPE 80 profile are analysed as an example for the adhesive Fischer FIS EM 390 S. In contrast, the analysis for the test specimens manufactured with the IPE 120 profile is carried out for the Weicon Easy-Mix HT 180 adhesive. The stiffness parameters for the test specimens with three stiffening elements are taken from the test curves for tests V3-F-IPE80-B and V2-W-IPE120-B shown in Sections 3.4.2 and 3.4.3.

The analysis of the stiffnesses in Table 4 shows that the global stiffness increases by a factor of approximately 3.1 for IPE 80, whereas the local stiffness increases by a factor of approximately 3.5. This difference is attributable to the definition of the two stiffness parameters. The local bending stiffness is evaluated in the constant-moment region between the load application points, where the three stiffened plate strips act essentially as parallel composite cross-sections; their contributions are therefore approximately additive, yielding a factor slightly above three, with the small excess resulting from the partially participating plate material between the stiffeners. The global stiffness, in contrast, also includes the flexibility of the support and connection region (end-plate joints to the HEM sections) as well as the load distribution across the wider panel. Since the connection details are not scaled with the number of stiffeners, the global stiffness does not scale linearly with the number of stiffeners, resulting in the slightly lower factor of 3.1.

By contrast, an analysis of the maximum machine forces achieved shows that these do not increase by a factor of three when three stiffeners are used. In the comparison shown, none of the test specimens failed during the test. Any loss of bond cannot therefore be cited as an explanation for the lower maximum machine force.

The results of tensile tests on specimens made from the steel components documented in section 3.1.1 offer a further, more well-founded explanation. According to these results, the mechanical properties, in particular the yield strength, differ to such an extent that this can account for the differences in machine forces once the yield strength is exceeded. Analysis of the results for each component separately shows that both the yield strength and the tensile strength of the components primed in red (specimen with three stiffeners) are 16 to 22 % lower than those of the equivalent components primed in grey (specimen with one stiffener). In particular, the strength of the stiffener profiles primed in red is significantly lower than that of the profiles primed in grey. Consequently, the unexpectedly small increase in the machine force corresponding to the yield limit lower than factor three can be explained by the lower strength of all components primed in red.

Table 4
Comparison of the evaluated global and local stiffnesses, as well as the limit of the elastic behaviour of the test specimens with one and three stiffeners, depending on the stiffener profile.

Number and type of stiffeners Adhesive	1 x IPE 80 Fischer FIS EM 390 S	3 x IPE 80	1 x IPE 120 Weicon Easy-Mix HT 180	3 x IPE 120
Global stiffness [kN/mm]	0.7	2.2	2.2	7.0
Local stiffness [kN/mm]	5.3	18.4	17.1	53.3
EI_{local} [10^{11} Nmm^2]	4.3	15.6	14.5	45.3
$F_{plasticity}$ [kN]	24.0	49.0	52.3	125.0

4.5. Conclusions

The key findings of the experimental investigations into the flexural behaviour of components stiffened by adhesive bonding can be summarised as follows:

- Bonding onto shop-primed steel is possible if the primer provides sufficient adhesion to the substrate and to the adhesive. This was shown for single-stiffener specimens. Adhesion tests on the delivered primer are therefore a prerequisite. In the three-stiffener series the primer quality was insufficient, and the bond surfaces were blasted (Sa 2½). On surfaces with sufficient adhesion (appropriate primer, sandblasted), up to three bonded stiffeners can reach their plastic load-bearing capacity without damage to the bonded joint.
- Provided that a suitable primer with sufficient load-bearing capacity is used, it is possible, using adhesive bonding, to attach several stiffening profiles to reinforce flat components in such a way that their plastic load bearing capacity can be utilised. The bonded joint is not damaged during the testing.
- The investigations of the influence of the adhesive show that an increase in the modulus of elasticity of the adhesive does not affect the local flexural stiffness. Consequently, adhesives of varying stiffness can be used to join stiff cross-sections. However, higher E-modules lead to an increase in stress peaks within the bonded joint and reduced robustness of the connection. Under the given manufacturing constraints, this results in reduced practical suitability of the process. Therefore, the choice of adhesive should primarily be based on the requirements for practical application and the creep behaviour of the adhesive.
- An increase in the moment of inertia of the stiffener profile results in an increase in the bending stiffness of both the composite cross-section and the overall system. However, the tests showed that a complete bond between the components could be achieved for both the stiffer and the less stiff profiles. In practice, however, it is important to keep in mind that, in addition to the moment of inertia of the stiffening profile, its own weight and the associated costs must also be taken into account. Shipyards can select the stiffening profile best suited to the application in question, taking these conditions into account.
- A change in the length of the stiffener does not affect the local bending stiffness of the composite cross-section. This finding is independent of the type of stiffener selected and the modulus of elasticity of the adhesive used. In terms of practical engineering applications, this implies that the experimentally determined results can be extrapolated to any span length. However, the influence of an increasing span length on the global stiffness of the composite cross-section must be taken into account.
- The global and local stiffnesses of the specimens are approximately linearly related to the number of stiffeners. No adverse scale effects were observed during the experimental investigations.

In summary, on surfaces providing sufficient adhesion—shop primer verified by adhesion testing, or primer locally removed by sandblasting to Sa 2½—and for the two adhesives investigated, the tests demonstrate that adhesive bonding is a technically viable method for attaching stiffening profiles (IPE 80, IPE 120, up to three per specimen) to flat steel structures in shipbuilding, allowing their full plastic bending capacity to be utilised without failure of the bonded joint. As a cold joining process, bonding avoids the thermal input of welding; the literature indicates that this reduces distortion and straightening effort, but this, together with manufacturing time, production cost and a direct comparison with welded reference specimens, was outside the scope of the present experimental programme. Durability aspects such as creep, temperature and moisture resistance, which are likewise relevant for shipbuilding applications, were not investigated within the project's time frame and are identified as a necessary next step (see Limitations). Key stiffness parameters relate approximately linearly to the number of stiffeners and are independent of span length, indicating that the load-bearing behaviour can be reliably scaled. Overall, under the tested conditions, adhesively bonded stiffening concepts represent a promising and practicable alternative to welded constructions for thin-walled maritime structures. These conclusions are based on quasi-static short-term tests. Component-scale durability and fatigue investigations, for which research in this field is still at an early stage, are required before the concept can be transferred into shipbuilding practice.

4.6. Limitations and future research need

The numerical model used for specimen and test-setup design is linear-elastic and does not include a failure criterion for the adhesive layer. A probabilistic assessment of adhesive bond failure, based on the material and geometry data of this study, is available in [64].

The study contains no parallel tests on welded specimens; the welded structure is used as a design reference only. Residual stresses, geometrical imperfections and fatigue behaviour of welded and bonded stiffeners were not measured.

This study focused on the short-term load-bearing behaviour of adhesively bonded stiffeners under quasi-static bending. Research on adhesively bonded steel structures at this scale is still at an early stage, particularly with regard to long-term performance. To the authors' knowledge, no durability data are available for component-scale bonded joints comparable to those investigated here. Owing to the time frame of the project, durability aspects, such as the effects of cyclic temperature changes, moisture and seawater exposure, salt spray, and sustained or cyclic loading on the bond line, on the primer-adhesive interface, and on the steel components, could not be examined in this study. Given the structural relevance of the bonded joints demonstrated here, component-scale durability and fatigue testing of adhesively bonded stiffeners, ideally combining accelerated ageing with representative mechanical loading, is identified as a necessary next step before the concept can be applied in shipbuilding practice.

Declaration of generative AI and AI-assisted technologies in the manuscript preparation process

During the preparation of this work the author(s) used [www.deepl.com and www.claude.ai] for translations linguistic refinement of the text. After using this tool/service, the author(s) reviewed and edited the content as needed and take(s) full responsibility for the content of the published article.

CRediT authorship contribution statement

Jannis Damm: Writing – original draft, Validation, Project administration, Methodology, Investigation, Formal analysis, Conceptualization, Writing – review & editing. **Peter Haase:** Writing – review & editing, Validation, Project administration, Methodology, Investigation, Formal analysis, Conceptualization. **Matthias Albiez:** Writing – review & editing, Supervision, Methodology, Funding acquisition, Conceptualization. **Thomas Ummenhofer:** Writing – review & editing, Supervision, Funding acquisition. **Sebastian Veller:** Writing – review & editing, Investigation, Funding acquisition.

Declaration of competing interest

The authors declare that they have no known competing financial interests or personal relationships that could have appeared to influence the work reported in this paper.

Acknowledgments

This research was supported by the German Federal Ministry of Economic Affairs and Climate Action through the German Federation of Industrial Research Associations (AiF) as part of the program for promoting industrial cooperative research project 01IF22351N of the German Association for Shipbuilding and Marine Technology (FSM).

Data availability

Data will be made available on request.

References

[1] Albiez M, Damm J, Ummenhofer T, et al. Hybrid joining of jacket structures for offshore wind turbines – Validation under static and dynamic loading at medium and large scale. Eng Struct 2022;252:113595. https://doi.org/10.1016/j.engstruct.2021.113595.
[2] Myslicki S, Kordy H, Kaufmann M, et al. Under water glued stud bonding fasteners for offshore structures. Int J Adhes Adhes 2020;98:102533.
[3] Mejri M, Cognard J-Y. Time-variant assessment for adhesively bonded assemblies with non-linear behaviour in naval applications. Sh Offshore Struct 2009;4(3):275–86.
[4] Maggiore S, Banea MD, Stagnaro P, et al. A review of structural adhesive joints in hybrid joining processes. Polym (Basel) 2021;13(22):3961.
[5] Mulcahy KR, Kilpatrick AFR, Harper GDJ, et al. Debondable adhesives and their use in recycling. Green Chem 2022;24(1):36–61.
[6] Mittal KL. Progress in Adhesion Adhesives,, 5. Newark: John Wiley & Sons, Incorporated; 2020.
[7] Veller S, Adam M, Hempel M, et al. Improving the recyclability of rare earth magnets in electrical motors by using debonding-strategies. Sustain Mater Technol 2025;45:e01586.
[8] Jarach N, Debondable DH. Recyclable and/or biodegradable naturally-based adhesives. In: Dunky M, Mittal KL, editors. Biobased Adhesives: Sources, Characteristics and Applications. 1st ed. Wiley; 2023. p. 427–61 [cited 2026 July 3]Available from: https://onlinelibrary.wiley.com/doi/10.1002/9781394175406.ch15.
[9] Perčić M, Ančić I, Vladimir N. Life-cycle cost assessments of different power system configurations to reduce the carbon footprint in the croatian short-sea shipping sector. Renew Sustain Energy Rev 2020;131:110028.
[10] Ndukwe A, Anumudu J, Ugwuegbu C, et al. Corrosion-protective coatings: an overview of self-healing and hybrid coating-advancements. Acta tech 2025;(56):159–86.
[11] American Bureau of Shipping (ABS). Guidance Notes on the Inspection, Maintenance and Application of Marine Coating Systems. Third Edition. American Bureau of Shipping (ABS); 2007. Houston, Texas.
[12] Weitzenböck JR. Adhesives in marine engineering. Oxford: Woodhead publ; 2012.
[13] Rodríguez-Dopico FJ, Carbas RJC, Borges CSP, et al. Combined effect of seawater and load on methacrylate adhesive. Heliyon 2023;9(4):e14751.
[14] Albiez M, Damm J, Ummenhofer T, et al. Hybrid joining of jacket structures for offshore wind turbines – determination of requirements and adhesive characterisation. Eng Struct 2022;259:114186. https://doi.org/10.1016/j.engstruct.2022.114186.
[15] Ellis TS, Karasz FE. Interaction of epoxy resins with water: the depression of glass transition temperature. Polym (Guildf) 1984;25(5):664–9.
[16] Bordes M, Davies P, Cognard J-Y, et al. Prediction of long term strength of adhesively bonded steel/epoxy joints in sea water. Int J Adhes Adhes 2009;29(6):595–608.
[17] Fay PA, Maddison A. Durability of adhesively bonded steel under salt spray and hydrothermal stress conditions. Int J Adhes Adhes 1990;10(3):179–86.
[18] Horton T, Spinks GM, Isles NA. Structural adhesive performance in marine environments. Polym Int 1992;28(1):9–17.
[19] Fröck L, Kaeding P, Kayser N. Adhesive technology in shipbuilding–opportunities and requirements. In: Da Silva LFM, Adams RD, editors. 8th International Conference on Structural Adhesive Bonding 2025 [Internet]. Cham: Springer Nature Switzerland; 2026. p. 173–85 [cited 2026 July 13]Available from: https://link.springer.com/10.1007/978-3-032-19022-2_10.
[20] Ortega-Iguña M, Akhavan-Safar A, Carbas RCJ, et al. Use of seawater to improve the static strength and fatigue life of bonded coated steel joints. Polym Degrad Stab 2022;206:110169.
[21] Momber AW, Fröck L, Marquardt T. Effects of accelerated ageing on the mechanical properties of adhesive joints between stainless steel and polymeric top coat materials for marine applications. Int J Adhes Adhes 2020;103:102699.
[22] Neuber HK, Klöppel NHK, Scheer. Beulwerte ausgesteifter Rechteckplatten. Kurventafeln zum direkten Nachweis der Beulsicherheit für verschiedene Steifenanordnungen und Belastungen. Z Angew Math Mech 1961;41(5). 226–226.
[23] Mahfuz H, Majumdar P, Saha M, et al. Integral manufacturing of composite skin-stringer assembly and their stability analyses. Appl Compos Mater (Dordr) 2004;11(3):155–71.

[24] Judaschke F. Grundlagen des Praktischen Schiffbaus. Nachdr. [der Ausg.] Berlin 1926. Bremen: Salzwasser-Verl; 2009.
[25] Zhang X, Li Y. Damage tolerance and fail safety of welded aircraft wing panels. AIAA J 2005;43(7):1613–23.
[26] Ackermann G. Die drillweiche, orthotrope, elastische platte als Berechnungsmodell für zweiachsig gespannte Filigrandecken. Beton Stahlbetonbau 1995;90(3):57–63.
[27] Singh DK, Pal P. Forced vibration analysis of stiffened lock gate structure. J Sound Vib 2021;510:116278.
[28] Singh DK, Pal P, Duggal SK. Free vibration analysis of stiffened lock gate structure. J Vib Eng Technol 2022;10(5):1779–91.
[29] Higgins A. Adhesive bonding of aircraft structures. Int J Adhes Adhes 2000;20(5):367–76.
[30] DIN Deutsches Institut für Normung e.V.. Schienenfahrzeuge 1: Grundlagen und Fertigungstechnologien, Fahrzeugaufbau und Sondereinrichtungen, Fahrgastraum, Fahrwerk. Berlin: Beuth Verlag; 2007.
[31] Deutsches Maritimes Zentrum e.V. (DMZ). Untersuchungen zum aktuellen internationalen Stand der Technik bezüglich Entwicklung und Anwendung von Klebeverbindungen in der Schiffsfertigung. Hamburg: Deutsches Maritimes Zentrum e.V. (DMZ); 2020.
[32] Hentinen Marrku. Boats and marine. Adhesive Bonding - Science, Technology and Applications. Oy, Espoo, Finland: Elsevier; 2021. https://linkinghub.elsevier.com/retrieve/pii/B9780128199541000058.
[33] Wium D, Lataire E, Belis J. Structural integration of glass in yacht superstructures through adhesive bonding – a numerical analysis. Mar Struct 2025;103:103834.
[34] Diez De Ulzurrun I, López F, Herreros MA, et al. Tests of deck-to-hull adhesive joints in GFRP boats. Eng Fail Anal 2007;14(2):310–20.
[35] Mouton L, Paboeuf S. Composite Superstructure Bonded to a Navy Ship Steel Hull. SAMPE Europe Conference Proceedings. Red Hook. NY: Curran Associates, Inc.; 2021.
[36] Siering KB, Schneider B, Klapp O. Standardisierung von Hochelastischen Aluminium-Stahl- und FVK-Stahl-Klebverbindungen für den Schiffbau (Abschlussbericht, IGF-Forschungsvorhaben 16764 N). Bremen, Hamburg: Forschungsvereinigung Schiffbau und Meerestechnik e.V. (FSM); 2014.
[37] Fröck L, Glück N, Nagel C. Eine wirtschaftliche Alternative zum Schweißen: Metall-Leitungen im Schiffbau klebtechnisch fügen (Teil 1). Adhaes Kleb Dicht 2015;59(10):42–7.
[38] Fröck L, Glück N, Nagel C. Den Bedingungen auf der Werft gewachsen: Metall-Leitungen im Schiffbau klebtechnisch fügen (Teil). Adhaes Kleb Dicht 2016;60(1–2):36–41.
[39] Blumentritt B, Glück N, Flügge W. Halterungen im Unterwasserbereich klebtechnisch fügen (Teil 1). Adhaes Kleb Dicht 2019;63(6):42–7.
[40] Blumentritt B, Glück N, Flügge W. Halterungen im Unterwasserbereich klebtechnisch fügen (Teil 2). Adhaes Kleb Dicht 2019;63(7–8):42–7.
[41] Anyfantis KN. Preliminary design assessment of an alternative repair method for corroded shear panels in ship hull structures. Ocean Eng 2019;188:106323.
[42] Goland M, Reissner E. The stresses in cemented joints. J Appl Mech 1944;11(1):A17–27.
[43] Hayashibara H, Iwata T, Ando T, et al. Degradation of structural adhesive bonding joints on ship exposure decks. J Mar Sci Technol 2020;25(2):510–9.
[44] Albiez M, Vallée T, Fricke H, et al. Adhesively bonded steel tubes — Part I: experimental investigations. Int J Adhes Adhes 2019;90:199–210.
[45] Albiez M, Vallée T, Ummenhofer T. Adhesively bonded steel tubes – Part II: numerical modelling and strength prediction. Int J Adhes Adhes 2019;90:211–24.
[46] Boretzki J, Albiez M, Myslicki S, et al. Hybrid grouted joints: Load bearing and failure behaviour under static, axial loading. Constr Build Mater 2024;413:134691.
[47] Myslicki S, Vallée T, Kaufmann M, et al. Harnessing the synergy of grout and adhesive: Numerical prediction of load capacity in hybrid composite joints. Int J Adhes Adhes 2024;130:103602.
[48] Myslicki S, Vallée T, Fricke H, et al. Hybrid grouted steel connections using adhesively bonded granules in the steel grout interface: development and validation of an innovative joining technique. Constr Build Mater 2024;414:134765.
[49] Boretzki J, Albiez M, Damm J, et al. Fatigue behaviour of hybrid grouted joints under axial loading. ce pap 2023;6(3–4):1151–6. https://doi.org/10.1002/cepa.2425.
[50] Boretzki J, Lemmrich L, Knape A, et al. Klebtechnischer Anschluss von Sekundärbauteilen bei Offshore-Bauwerken. Adhaes Kleb Dicht 2023;67(4):34–9.
[51] Albiez M, Boretzki J, Ummenhofer T. Adhesive bonding of secondary steel components for offshore wind turbines. ce pap 2023;6(3–4):959–63.
[52] Mantik J, Glienke R, Dörre M, et al. Aktuelle erkenntnisse zum Einsatz von Klebstoff in vorgespannten Schraubenverbindungen unter Berücksichtigung von Fertigungseinflüssen. Stahlbau 2024;93(5):306–20.
[53] Evers T, Vallée T, Specht U, et al. Strengthening the grid: hybrid-bonded bolted joints for retrofitting weathered power-line structures. J Adhes 2025:1–30.
[54] Kasper Y, Albiez M, Ciupack Y, et al. Verstärkung von ermüdungsbeanspruchten Stahlbauteilen mit aufgeklebten CFK- lamellen – Teil 1: Grundlagen und Materialien. Bauingenieur 2020;95(03):79–84.
[55] Kasper Y, Albiez M, Ummenhofer T, et al. Verstärkung von ermüdungsbeanspruchten Stahlbauteilen mit aufgeklebten CFK-Lamellen – Teil 2: Experimentelle Rissfortschrittsuntersuchungen. Bauingenieur 2020;95(05):166–73.
[56] Kasper Y, Albiez M, Ummenhofer T, et al. Application of toughened epoxy-adhesives for strengthening of fatigue-damaged steel structures. Constr Build Mater 2021;275:121579.
[57] Damm J, Ummenhofer T, Albiez M, et al. Experimental and numerical investigation of the damping properties of adhesively bonded tubular steel joints. J Adhes 2023;99:2191–221. https://doi.org/10.1080/00218464.2023.2178909.
[58] Damm J, Albiez M. Damping properties of large-scale overlap joints bonded with epoxy hybrid resin or polyurethanes: experimental characterisation and analytical description. Polym (Basel) 2023;15(5):1102.
[59] Damm J, Ummenhofer T, Albiez M. Influence of damping properties of adhesively bonded joints on the dynamic behaviour of steel structures: numerical investigations. J Adhes 2022;98(7):934–62. https://doi.org/10.1080/00218464.2020.1865161.
[60] Feyz Bashipour A, Keshavarzi A, Saeidi Googarchin H. Bio-inspired hybrid aluminum/CFRP sandwich structure: a ductile containment strategy for energy absorption. Mater Des 2026;267:116366.
[61] Baratian Sani Devin A, Keshavarzi A, Saeidi Googarchin H. Harnessing predictable failure: a bio-inspired adhesively bonded Al/CFRP hybrid structure with guided crushing for enhanced crashworthiness under oblique loading. Mater Des 2026;262:115461.
[62] Ghasempoor H, Keshavarzi A, Saeidi Googarchin H. Machine learning-enhanced prediction of energy absorption in AL/CFRP hybrid tubes under oblique compression. Mech Adv Mater Struct 2026;33(1):2627539.
[63] Veller S, Vallée T, Damm J, et al. Adhesive bonding of shop-primed steel in shipbuilding applications (submitted). Int J Adhes Adhes [Internet] 2026. doi: to be determined.
[64] Damm J, Albiez M, Haase P, et al. Aufgeklebte profile zur Versteifung von flächigen Bauteilen in maritimen Strukturen (KlebProfi). Hamburg: Forschungsvereinigung Schiffbau und Meerestechnik e.V. (FSM) 2026. Report No.: FSM-Bericht 11/2026.
[65] Kunststoffe - Bestimmung der Zugeigenschaften - Teil 1: Allgemeine Grundsätze. Berlin: Beuth Verlag; 2019.
[66] DIN EN ISO 4624: Beschichtungsstoffe - Abreißversuch zur Bestimmung der Haftfestigkeit. Berlin: Beuth Verlag; 2023.
[67] DIN EN 10025-1: Warmgewalzte Erzeugnisse aus Baustählen – Teil 1: Allgemeine technische Lieferbedingungen. Berlin: Beuth Verlag; 2005.
[68] DIN EN ISO 6892-1: Metallische Werkstoffe – Zugversuch – Teil 1: Prüfverfahren bei Raumtemperatur. Berlin: Beuth Verlag; 2020.
[69] Prüfung metallischer Werkstoffe – Zugproben. Berlin: Beuth Verlag; 2022.
[70] Seong W-J, Na S-J. Systematization of heat straightening process of stiffened plate by surface flattening. J Mater Process Technol 2022;299:117333.
[71] Long H, Gery D, Carlier A, et al. Prediction of welding distortion in butt joint of thin plates. Mater Des 2009;30(10):4126–35.
[72] Deng D, Murakawa H. Prediction of welding distortion and residual stress in a thin plate butt-welded joint. Comput Mater Sci 2008;43(2):353–65.

[73] Tuswan Zubaydi A, Budipriyanto A, et al. Comparative Study on Ferry Ro-Ro's Car Deck Structural Strength by Means of Application of Sandwich Materials: Proceedings of the 3rd International Conference on Marine Technology [Internet]. Surabaya, Indonesia: SCITEPRESS - Science and Technology Publications; 2018 [cited 2026 May 19]. p. 87–96. Available from: https://www.scitepress.org/DigitalLibrary/Link.aspx?doi=10.5220/0008542800870096.
[74] Det Norske Veritas (DNV). Rules for classification: Ships. Høvik, Norway: DNV; 2022.
[75] DIN EN 408: Holzbauwerke - Bauholz für tragende Zwecke und Brettschichtholz - Bestimmung einiger Physikalischer und Mechanischer Eigenschaften. Berlin: Beuth Verlag; 2023.